



A SPATIAL NONLINEAR MATHEMATICAL MODEL OF MALARIA TRANSMISSION DYNAMICS USING VECTOR CONTROL STRATEGIES

CHARITY JUMAI ALHASSAN, AND KENNETH OJOTOGBA ACHEMA*

ABSTRACT. Malaria is one of the serious life-threatening diseases with negative effects on both the social and economic aspects of human life. Researching into its curtailment or eradication is necessary for elevating human health and social-economic status. In this regard, this study focuses on the spatial non-linear mathematical model to investigate how vector control strategies are correlated with the dynamics of malaria transmission. The study employs a non-linear partial differential equations (NPDE) mathematical model to investigate malaria transmission. The model system incorporates human (host), mosquito (vector), and invasive alien plant populations. Some applicable epidemiological mathematical analyses were carried out on the model system, such as critical points, stability, the basic reproduction number, local asymptotic stability (LAS), bifurcation, global asymptotic stability (GAS), wave speed, and numerical analyses using relevant data were extensively analysed. Using the sharp threshold conditions imposed on the basic reproduction number, we were able to show that the model exhibited the backward bifurcation phenomenon and the DFE was shown to be globally asymptotic stable (GAS) under certain conditions. It was found that the invasive alien plants have significant effects on malaria transmission. This study suggests that mosquito repellent plants should be planted around the human environment to replace the invasive plants so as to reduce mosquito shelters and feeding opportunities for mosquitoes.

1. INTRODUCTION

Malaria is a life-threatening illness that affects millions of people all over the world (WHO, 2021), despite that there are new scientific research innovations for curtailing and preventing the vector, such as insecticide spray and insecticide-treated bed nets (Raghavendra et al. 2011; Ranson et al. 2011). For instance, in so many parts of African countries, the disease remains endemic and severe, and even though the mortality rates have drastically reduced in 2013, it was estimated that about 855,000 people died of malaria (Cjl et al., 2014). However, with the application of insecticide-treated bed nets control measures, there is a drastic decline in malaria transmission (WHO, 2022). In 2017, it was estimated that only 435,000 deaths occurred, as against 855,000 in 2013.

Key words and phrases. mathematical model, malaria; spatial; reproduction number; invasive alien plant; travelling wave.

Received: June 06, 2024. Accepted: August 06, 2024. Published: September 30, 2024.

*Corresponding author.

Malaria infection begins when an infected female *Anopheles* mosquito bites a susceptible human. As a result, the parasites in the form of sporozoites enter or are injected into the bloodstream and then transferred from the susceptible individuals into exposed individuals. Malaria infection has an incubation period of 7 to 30 days after an infective female *Anopheles* mosquito bites a susceptible human and its symptoms include diarrhea, fever, chills, and vomiting to mention a few, and can also occur for years if not treated on time. Recently, the World Malaria Report (WMR) reported 241 million cases of malaria in 2020, which is higher than the previous year's (2019) figure of 227 million cases of malaria. However, in 2020, the estimated number of malaria deaths stood at 627,000 - an increase of 69,000 deaths over the previous year (2019) was recorded. It is worth noting that about two-thirds of these deaths (47,000) were due to disruptions during the COVID-19 pandemic, while the remaining one-third of deaths (22,000) reflects a recent change in WHO's methodology for calculating malaria mortality (regardless of COVID-19 disruptions)(WHO, 2022). Even though African countries accounted for almost half of the disease burden and more than half of the malaria deaths worldwide, Nigeria has the highest share of the disease burden (31.9%) followed by the Democratic Republic of Congo (13.2%), the United Republic of Tanzania (4.1%) and Mozambique (3.8%)(WHO, 2022).

Malaria infections are normally prevented by the following four scientific ways, which include insecticide-treated bed nets (ITNS), indoor residual spraying, and intermittent-preventive treatment, while artemisinin-based combination therapy (ACT) is used for the treatment of uncomplicated malaria (Mack and Smith 2011). Vaccination has proved over time as a preventive measure for malaria disease. In October 2021, the World Health Organisation (WHO) recommended broad use of the RTS, S/AS01 malaria vaccine among children living in regions with moderate to high *plasmodium falciparum* malaria transmission. The vaccine has been shown to significantly reduce malaria, and deadly severe malaria, among young children (WHO, 2021). This was as a result of the malaria report in 2020 that the African Region had 95% of malaria cases and 96% of malaria deaths. Children under 5 years accounted for about 80% of all malaria deaths in the region.

Environmental management became paramount over decades to obtain a sound and environmentally friendly ecosystem. The environmental protection agency (EPA) programme was highly successful as a result of environmental measures for the control of both *falciparum* and *vivax plasmodium* as parts of mosquito larvae in the early 1900s. The work was based on Watson in Malaysia, which showed the necessity of environmental modification by selective clearing of forests that harbour mosquitoes (Nkya et al. 2014). The world health organisation (WHO) uses dichlorodiphenyltrichloroethane (DDT) as one of the major control mechanisms for eradicating malaria in 1956-1967, and it was not expensive to purchase and use, and highly recommended insecticides as the residual house spraying which was highly effective and promised an end to malaria. The campaign for DDT failed due to its environmental persistence and effects led to its being banned by the government of the USA in 1972. Stone et al. (2018) presented another promised method of eradicating malaria due to changes in vegetation structure and composition, or as a result of deforestation (Villa et al. 2011; Zhu et al. 2015; Hien et al. 2016; Shackleton et al. 2017). In Africa, invasive alien plants are now one of the major problems, and in other African regions, where they have negative effects on health, water and other natural resources, and also pasture production. The invasive alien plants are capable of affecting human resources in two ways. First of all, both male and female mosquitoes need sugar and honeydew for their survival and also obtained from floral sources. And secondly, the invasive plants serve as breeding and resting sites for adult mosquitoes, thus enhancing

malaria vector multiplication (Kroeger et al. 2013; Muturi et al. 2015; Davis et al. 2016; Gardner et al. 2017; Muller et al. 2017; Stone et al. 2018).

Mathematical models have become significant tools for understanding the transmission of malaria infections and also offer control measures that will enable health professionals to overcome the disease (Diabate et al., 2022; Koutou et al., 2023). However, Artzy et al. (2010) formulated a mathematical model for the transmission intensity and drug resistance in malaria population dynamics and underscore that climate change and drug resistance can interact and need not be considered as alternative explanations for trends in disease incidence in this region. Julius et al. (2014) extended the work of Tumwine et al. (2017) model in which they divided the infected human population into individuals infected with drug-sensitive and resistance. Their findings were that the basic reproduction number was obtained in terms of the demographic and epidemiological parameters. It is noted from this threshold parameter that the effectiveness of treatment for the sensitive parasite plays a crucial role in the spread of the disease and the emergence of drug resistance against the most common and affordable anti-malarial poses a key obstacle to malaria control.

A mathematical model for the in-host dynamics of malaria and the effects of treatment was proposed by Zadoki et al. (2017). It was found that the infection rate of merozoites, the rate of sexual reproduction in gametocytes, and the burst size of both hepatocytes and erythrocytes are more sensitive parameters for the onset of the disease. It was also reported that a treatment strategy using highly effective drugs against such parameters can reduce malaria transmission. Resmawan (2017) provides numerical simulations to show the effectiveness of vaccines and anti-malaria drugs in humans to suppress the rate of transmission of disease. It was assumed that humans in the susceptible class could move into the recovering class due to vaccination. The simulation results showed that the increase in vaccine effectiveness and anti-malaria drugs in humans can reduce the reproduction numbers so that within a certain time the disease will vanish from the population. Titus et al. (2018) modelled and studied the in-host plasmodium falciparum malaria subject to malaria vaccines was formulated and analysed. An efficacious pre-erythrocytic vaccine was shown to greatly reduce the severity of clinical malaria. Based on the normalized forward sensitivity index technique, the average number of merozoites released per bursting blood schizont was shown to be the most sensitive parameter in the model. More so, Takoutsing et al. (2019) investigated the malaria dynamics model of a within-host and with periodic anti-malaria treatment. They found that eradication is possible under periodic regimens. A Spatio-temporal model, using Diffusion-Reaction equations to describe how the drug duration and efficiency can affect the parasite dispersal was also derived. In this work, we propose a spatial non-linear mathematical model on the impact of vector control strategies on the dynamics of malaria transmission. This work would result in helping policy-makers to make decisions on how to reduce or eliminate invasive alien plants in the human environment without compromising environmental sustainability and global warming disasters to human lives.

The organisation of this paper is as follows. The model is formulated in Section 2. The analyses of the formulated model and its numerical simulations are carried out in Section 3 and Section 4 respectively. The wave equation analyses and its numerical experiments are carried out in Section 5. Discussion and conclusion are presented in Section 6 and 7 respectively.

2. MODEL FORMULATION

In this section, we shall formulate mathematical model based on the biological paper presented by stone et al. (2018) as follows.

2.1. Assumptions of the model equations. For proper understanding and formulation of system of equations in this study, we present the following assumptions:

- (H_1) Invasive alien plants close to human population is capable of providing shelter for a high density of the mosquito population.
- (H_2) Mosquitoes migrate from vegetation/invasive alien plants to human environment due to their proximity to human habitat (Stone et al. 2018).
- (H_3) We also assume that recovered humans lost immunity and become susceptible.
- (H_4) There is a spatial movement of vectors from the invasive alien plants sites at the borders of the community.
- (H_5) We consider that susceptible, exposed and infected vectors have the same coefficients of diffusion, D and of advection, K , because the disease has no effect on vector movement (Vanessa and Norberto 2019);
- (H_6) We assumed that the distance measures from where the invasive plants are to human habitat can be covered by the vectors especially Anopheles mosquitoes.
- (H_7) We describe the spatial spread of the disease by the diffusion and advection of the vectors only, disregarding the large-scale spatial movements of the human population. These insects usually feed on hosts at night, so humans need to sleep in their houses in villages in order to become infected. Hence, we do not assume local dissemination by human movements.
- (H_8) To make the population constant over time, we assumed that the recruitment rate is the same as those that died naturally and due to infection (Vanessa and Norberto 2019).

2.2. Model variables and parameters. The variables and the parameters of our formulated model are given in Table 1 below.

2.3. Descriptions of the model equations. In order to provide a quick understanding of our proposed model, we will briefly describe each compartment of our proposed model as follows. The susceptible human recruitment rate is denoted by μ_h , which is the same as the natural death rate of all the compartments. The population is increased by the recovered persons that lost immunity and the disease induced death rate, while the population is decreased by those that had contact with the infected mosquitoes and became exposed and those that died naturally. The exposed human population/compartment is made up of those that had contact with infected mosquitoes and is decreased by those that became infected after some few days of exposure to mosquito bites and those that died naturally. The infected human compartment is formed by exposed individuals that have malaria parasites in their blood stream beyond the disease incubation period. The population is decreased by recovered individuals, those that died due to infection and those that died natural death. The recovered human compartment is formed by those that recovered from the disease and is decreased by those that lost immunity and those that died naturally. The invasive alien plants population is logistically modelled. The population is increased by the plant's growth rate and is decreased by the plant's reduction/control rate, h . The susceptible mosquito compartment flight behaviour is described by the PDE, $D \frac{\partial^2 S_m}{\partial x^2} - K \frac{\partial S_m}{\partial x}$ where the D and K represent the diffusion and advection movement of the mosquitoes

TABLE 1. Description of model variables and parameters

Variable/Parameter	Interpretation
$S_h(t)$	Susceptible human population at time t
$E_h(t)$	Exposed human population at time t
$I_h(t)$	Infected human population at time t
$R_h(t)$	Recovered human population at time t
$S_m(t)$	Susceptible mosquito population at time t
$E_m(t)$	Exposed mosquito population at time t
$I_m(t)$	Infected mosquito population at time t
$P(t)$	Plant population at time t
b	Number of bite per mosquito/vector
D	The coefficient of diffusion
K	The coefficient of advection
q_h	Rate at which exposed human population become infected
v_h	Recovered rate of infected individual
α_h	Recovery rate of human
h	Control rate of invasive alien plants
θ_m	recruitment rate of mosquitoes from the density of invasive plants into the general susceptible mosquito
μ_h	Recruitment rate of susceptible human and natural death rate of humans
δ_h	Disease induced death rate
g	Growth rate of invasive alien plants
K_p	Plant carrying capacity
μ_m	Recruitment rate of susceptible mosquitoes and natural death rate of mosquitoes
$\lambda_h(t)$	Force of infection for humans
$\lambda_m(t)$	Force of infection for vectors
β_{hv}	probability of malaria transmission from infectious humans to susceptible mosquitoes
β_{mh}	probability of malaria transmission from infected vectors to susceptible humans
ϵ	Availability of bed-nets
γ	Efficacy of bed-nets

respectively. The susceptible mosquito is formed by the birth rate of μ_m and those that migrated from the invasive plants with the rate, θ_m . The population is decreased by those that had contact with the infected humans and those that died naturally. The exposed mosquito compartment flight behaviour is described by the PDE, $D \frac{\partial^2 E_m}{\partial x^2} - K \frac{\partial E_m}{\partial x}$ where the D and K represent the diffusion and advection movement of the mosquitoes. The exposed mosquito is formed by the vector force of infection, λ_m and is decreased by those that developed infection by the rate, q_m and those that died naturally, μ_m . The infected mosquito compartment flight behaviour is described by the PDE, $D \frac{\partial^2 I_m}{\partial x^2} - k \frac{\partial I_m}{\partial x}$ where the D and K represent the diffusion and advection movement of the mosquitoes respectively. The

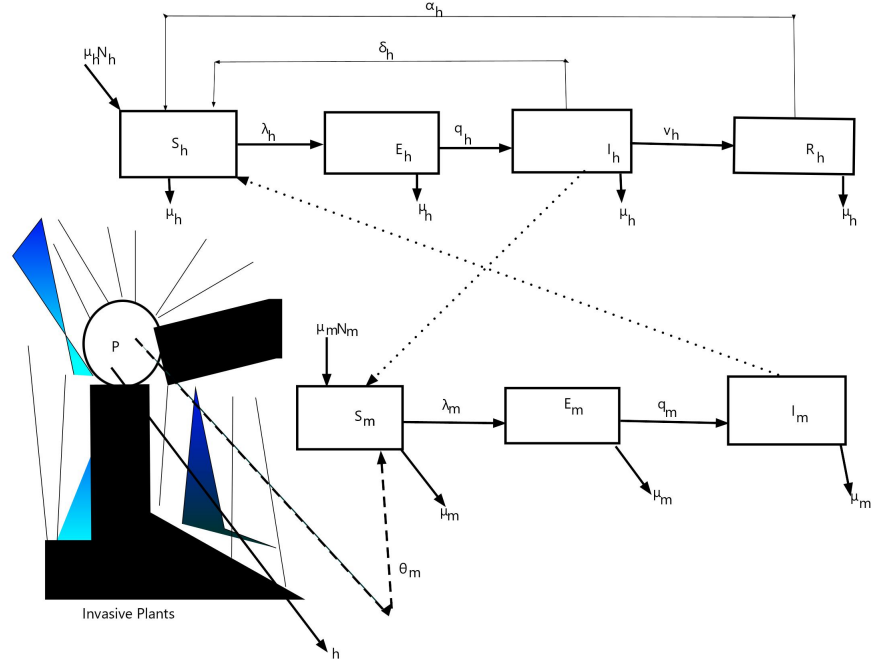


FIGURE 1. Schematic diagram of the model (1) with given values of λ_h and λ_m

infected mosquito's compartment is formed by the exposed mosquitoes that developed infection at the rate q_m and is decreased by those that died naturally, μ_m .

2.4. Model equations. Keeping track of the above assumptions, variables, parameter descriptions, and schematic diagram, the formulated model equations are given by

$$\begin{aligned}
 \frac{\partial \bar{S}_h}{\partial t} &= \mu_h \bar{N}_h + \delta_h \bar{I}_h + \alpha_h \bar{R}_h - \lambda_h \bar{S}_h - \mu_h \bar{S}_h \\
 \frac{\partial \bar{E}_h}{\partial t} &= \lambda_h \bar{S}_h - (q_h + \mu_h) \bar{E}_h \\
 \frac{\partial \bar{I}_h}{\partial t} &= q_h \bar{E}_h - (\delta_h + \mu_h + v_h) \bar{I}_h \\
 \frac{\partial \bar{R}_h}{\partial t} &= v_h \bar{I}_h - (\mu_h + \alpha_h) \bar{R}_h \\
 \frac{\partial \bar{P}}{\partial t} &= g(1 - \frac{\bar{P}}{K_P}) \bar{P} - h \bar{P} \\
 \frac{\partial \bar{S}_m}{\partial t} &= D \frac{\partial^2 \bar{S}_m}{\partial x^2} - K \frac{\partial \bar{S}_m}{\partial x} + \mu_m \bar{V} + \theta_m P - \lambda_m \bar{S}_m - \mu_m \bar{S}_m \\
 \frac{\partial \bar{E}_m}{\partial t} &= D \frac{\partial^2 \bar{E}_m}{\partial x^2} - K \frac{\partial \bar{E}_m}{\partial x} + \lambda_m \bar{N}_m - (q_m + \mu_m) \bar{E}_m \\
 \frac{\partial \bar{I}_m}{\partial t} &= D \frac{\partial^2 \bar{I}_m}{\partial x^2} - K \frac{\partial \bar{I}_m}{\partial x} + q_m \bar{E}_m - \mu_m \bar{I}_m
 \end{aligned} \tag{2.1}$$

Where,

$$\lambda_h = (1 - \epsilon\gamma)\beta_{hm}\frac{b\bar{I}_m}{\bar{N}_h}, \lambda_m = (1 - \epsilon\gamma)\beta_{mh}\frac{b\bar{I}_h}{\bar{N}_h}, 0 < \epsilon < 1, 0 < \gamma < 1 \quad (2.2)$$

with the initial and boundary conditions:

$$\begin{aligned} \bar{S}_h(0, x) &> 0, \bar{E}_h(0, x) \geq 0, \bar{I}_h(0, x) \geq 0, \bar{R}_h(0, x) \geq 0 \\ \bar{P}(0, x) &\geq 0, \bar{S}_m(0, x) > 0, \bar{E}_m(0, x) \geq 0, \bar{I}_m(0, x) \geq 0, \\ \bar{S}_{mx}(t, 0) &= 0, \bar{S}_m(t, 1) = 1, \bar{E}_{mx}(t, 1) = 0, \\ \bar{E}_m(t, 0) &= 0, \bar{I}_{mx}(t, 0) = 0, \bar{E}_m(t, 0) = 0. \end{aligned}$$

where D and K are the coefficients of diffusion and advection of the mosquitoes respectively.

The total human population is $\bar{N}_h = \bar{S}_h + \bar{E}_h + \bar{I}_h + \bar{R}_h$, and the total population is given by $\bar{N}_m = \bar{S}_m + \bar{E}_m + \bar{I}_m$

We will normalize model (2.1) using the following changed variables with the following scaling parameters:

$$S_h = \frac{\bar{S}_h}{\bar{N}_h}, E_h = \frac{\bar{E}_h}{\bar{N}_h}, I_h = \frac{\bar{I}_h}{\bar{N}_h}, R_h = \frac{\bar{R}_h}{\bar{N}_h}, P = \frac{\bar{P}}{\bar{P}^*}, S_m = \frac{\bar{S}_m}{\bar{N}_m}, E_m = \frac{\bar{E}_m}{\bar{N}_m} \text{ and } I_m = \frac{\bar{I}_m}{\bar{N}_m}.$$

Substituting the re-scaled variables, together with their respective changes in derivatives, into model (2.1), after several algebraic calculations, yields the following normalized system:

$$\begin{aligned} \frac{\partial S_h}{\partial t} &= \mu_h(1 - S_h) + \delta_h I_h + \alpha_h R_h - k_1 S_h I_m \\ \frac{\partial E_h}{\partial t} &= k_1 S_h I_m - (q_h + \mu_h) E_h \\ \frac{\partial I_h}{\partial t} &= q_h E_h - (\delta_h + \mu_h + v_h) I_h \\ \frac{\partial R_h}{\partial t} &= v_h I_h - (\mu_h + \alpha_h) R_h \\ \frac{\partial P}{\partial t} &= g(1 - P)P - hP \\ \frac{\partial S_m}{\partial t} &= D \frac{\partial^2 S_m}{\partial x^2} - K \frac{\partial S_m}{\partial x} + \mu_m(1 - S_m) + \theta_m c P - k_2 I_h S_m \\ \frac{\partial E_m}{\partial t} &= D \frac{\partial^2 E_m}{\partial x^2} - K \frac{\partial E_m}{\partial x} + k_2 I_h S_m - (q_m + \mu_m) E_m \\ \frac{\partial I_m}{\partial t} &= D \frac{\partial^2 I_m}{\partial x^2} - K \frac{\partial I_m}{\partial x} + q_m E_m - \mu_m I_m \end{aligned} \quad (2.3)$$

where

$$k_1 = (1 - \epsilon\gamma)\beta_{hm}b\frac{\bar{N}_m}{\bar{N}_h}, k_2 = (1 - \epsilon\gamma)\beta_{mh}b, c = \frac{k_p}{\bar{N}_m}, 0 < \epsilon < 1, 0 < \gamma < 1.$$

with the initial and boundary conditions:

$$\begin{aligned} S_h(0, x) &> 0, E_h(0, x) \geq 0, I_h(0, x) \geq 0, R_h(0, x) \geq 0 \\ P(0, x) &\geq 0, S_m(0, x) > 0, E_m(0, x) \geq 0, I_m(0, x) \geq 0, \\ S_{mx}(t, 0) &= 0, S_m(t, 1) = 1, E_{mx}(t, 1) = 0, \\ E_m(t, 0) &= 0, I_{mx}(t, 0) = 0, E_m(t, 0) = 0. \end{aligned}$$

Now, from the normalization and re-scaling carried out, we can now uncouple the system to become

$$\begin{aligned} \frac{\partial e_h}{\partial t} &= \lambda_h(1 - e_h - i_h - r_h) - (q_h + \mu_h)e_h \\ \frac{\partial i_h}{\partial t} &= q_h e_h - (\delta_h + v_h + \mu_h)i_h \\ \frac{\partial r_h}{\partial t} &= v_h i_h - (\mu_h + \alpha_h)r_h \\ \frac{\partial P}{\partial t} &= g(1 - P)P - hP \\ \frac{\partial e_m}{\partial t} &= D \frac{\partial^2 e_m}{\partial x^2} - K \frac{\partial e_m}{\partial x} + \lambda_m(1 - e_m - i_m) - (q_m + \mu_m)e_m \\ \frac{\partial i_m}{\partial t} &= D \frac{\partial^2 i_m}{\partial x^2} - K \frac{\partial i_m}{\partial x} + q_m e_m - \mu_m i_m \end{aligned} \tag{2.4}$$

3. MODEL ANALYSIS

We first considered and studied the dynamics of the homogeneous model. The spatial homogeneous model corresponding to system (2.3) is given by

$$\begin{aligned} \frac{dS_h}{dt} &= \mu_h(1 - S_h) + \delta_h I_h + \alpha_h R_h - k_1 I_m S_h \\ \frac{dE_h}{dt} &= k_1 I_m S_h - (q_h + \mu_h)E_h \\ \frac{dI_h}{dt} &= q_h E_h - (\delta_h + \mu_h + v_h)I_h \\ \frac{dR_h}{dt} &= v_h I_h - (\mu_h + \alpha_h)R_h \\ \frac{dP}{dt} &= g(1 - P)P - hP \\ \frac{dS_m}{dt} &= \mu_m(1 - S_m) + \theta_m cP - k_2 I_h S_m \\ \frac{dE_m}{dt} &= k_2 I_h S_m - (q_m + \mu_m)E_m \\ \frac{dI_m}{dt} &= q_m E_m - \mu_m I_m \end{aligned} \tag{3.1}$$

3.1. Basic properties of the spatial homogeneous equations. Let $N_h(t) = S_h(t) + E_h(t) + I_h(t) + R_h(t)$ be the total population of human at time, t . Also, let $N_m(t) = S_m(t) + E_m(t) + I_m(t)$ be the total population of mosquitoes at time, t . Let P be the plants population at time, t . The feasible region of the model (3.1) is given by

$$\Omega = \{(S_h + E_h + I_h + R_h, P, S_m + E_m + I_m) \in \mathbb{R}_+^8 : S_h + E_h + I_h + R_h = 1; P = \frac{g}{h}; S_m + E_m + I_m = 1, S_h > 0, E_h \geq 0, I_h \geq 0, R_h \geq 0; P > 0; S_m > 0, E_m \geq 0, I_m \geq 0\}$$

3.2. Disease free equilibrium (DFE) analysis. In this section, we shall carry-out a qualitative analysis of the model equations as follows.

3.2.1. Case I: When there are invasive plants in human environment. Disease free-equilibrium (DFE) corresponding to the presence of invasive alien plants is given by

$$\begin{aligned} E_1 &= (S_h^*, E_h^*, I_h^*, R_h^*, P^*, S_m^*, E_m^*, I_m^*) \\ &= (1, 0, 0, 0, \frac{(g-h)}{g}, \frac{\mu_m g + \theta_m c(g-h)}{\mu_m g}, 0, 0) \end{aligned} \quad (3.2)$$

for $g - h > 0$ (which denotes the higher growth rate of plants than control rate).

Even when $g = h$, there is still a DFE. In this case, the DFE becomes a DFE without invasive plants (i.e. the equilibrium E_1 becomes $E_2 = (1, 0, 0, 0, 0, 1, 0, 0)$).

The biological implication of this equilibrium, E_1 , is that the DFE state in the presence of invasive plants and susceptible mosquitoes is possible for malaria to be eradicated from the local community even when the invasive plants are present in the target community.

3.2.2. Basic Reproduction number (R_0). To calculate the effective reproduction number, we divide system (3.1) into appearance of infection and transfer of infection as matrix $F_i(x)$ and $V_i(x)$ respectively as follows:

$$\begin{aligned} F &= \begin{pmatrix} 0 & 0 & 0 & (1 - \epsilon\gamma)\beta_{hm}b \\ 0 & 0 & 0 & 0 \\ 0 & \frac{V_h g + K_p \theta_m (g-h)}{g(\xi_m + \mu_m)}(1 - \epsilon\gamma)\beta_{hm}b & 0 & 0 \\ 0 & 0 & 0 & 0 \end{pmatrix}, \\ V &= \begin{pmatrix} q_h + \mu_h & 0 & 0 & 0 \\ -q_h & \delta_h + \mu_h + v_h & 0 & 0 \\ 0 & 0 & q_m + \xi_m + \mu_m & 0 \\ 0 & 0 & -q_m & \xi_m + \mu_m \end{pmatrix} \\ V^{-1} &= \begin{pmatrix} \frac{1}{q_h + \mu_h} & 0 & 0 & 0 \\ \frac{q_h}{(q_h + \mu_h)(v_h + \delta_h + \mu_h)} & \frac{1}{\delta_h + \mu_h + v_h} & 0 & 0 \\ 0 & 0 & \frac{1}{q_m + \xi_m + \mu_m} & 0 \\ 0 & 0 & \frac{q_m}{(\mu_m + \xi_m)(q_m + \mu_m + \xi_m)} & \frac{1}{(\mu_m + \xi_m)} \end{pmatrix} \end{aligned}$$

Therefore, the spectral radius of FV^{-1} gives the effective reproduction number as shown below.

$$R_{01} = \sqrt{\frac{k_1 k_2 k_3 q_m (q_m + \mu_m)}{\mu_m (q_h + \mu_h) (v_h + \delta_h + \mu_h) (q_m + \mu_m) (q_m + \mu_m)}}$$

where $k_1 = (1 - \epsilon\gamma)\beta_{hm}b$, $k_2 = (1 - \epsilon\gamma)\beta_{mh}b$, $k_3 = \frac{\mu_m g + \theta_m c(g-h)}{\mu g}$

3.2.3. Case II: When there are no invasive alien plants in human environment. Here, we recompute the basic reproduction number of system (3.1), where there are no invasive alien plants. Equilibrium, E_2 , is used in this case and is given by

$$\begin{aligned} E_2 &= (S_h^+, E_h^+, I_h^+, R_h^+, P^+, S_m^+, E_m^+, I_m^+) \\ &= (1, 0, 0, 0, 0, 1, 0, 0) \end{aligned} \quad (3.3)$$

3.2.4. *Analysis of basic reproduction number (R_0).* Following the approach in Van den Driessche and Watmough (2008), the approach used above, we calculated the effective reproduction number of the homogeneous system to be

$$R_{02} = \sqrt{\frac{k_1 k_2 q_m (q_m + \mu_m)}{\mu_m (q_h + \mu_h) (v_h + \delta_h + \mu_h) (q_m + \mu_m) (q_m + \mu_m)}}$$

where $k_1 = (1 - \epsilon\gamma)\beta_{hm}b$, $k_2 = (1 - \epsilon\gamma)\beta_{mh}b$.

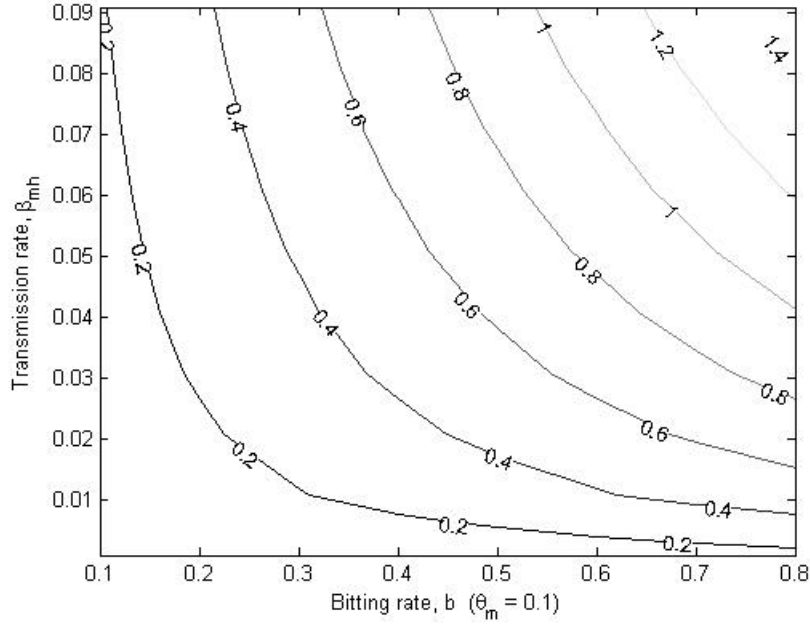


FIGURE 2. Contour plot of R_{01} for $\theta_m = 0.1$

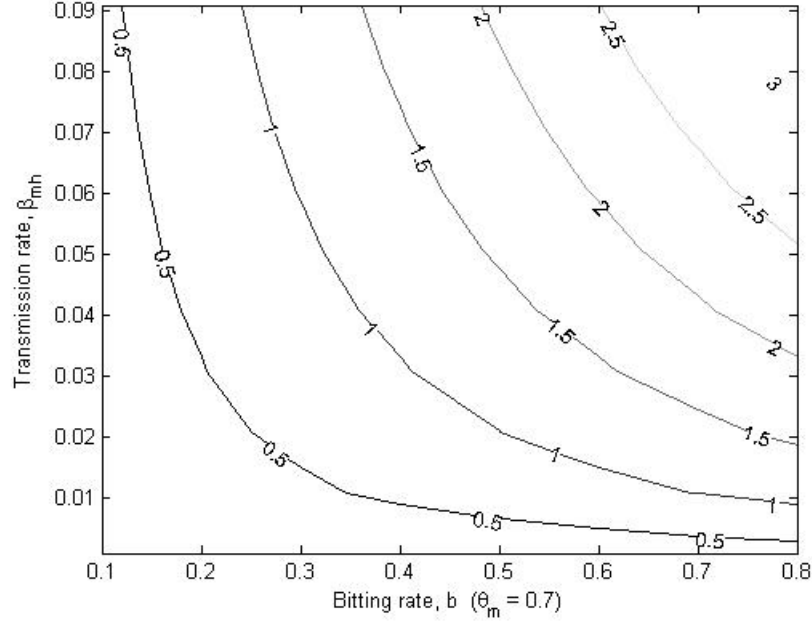
3.3. **Local asymptotic stability (LAS) of E_1 equilibrium.** The local asymptotic stability (LAS) of the equilibrium, E_1 is obtained using Theorem 1.

Theorem 3.1. *For $R_{01}^2 < 1$, E_1 is locally asymptotically stable and unstable if otherwise.*

Proof. Linearizing the spatial homogeneous model (3.1) with the corresponding equilibrium, E_1 , we obtained the following:

$$J(E_1) = \begin{pmatrix} -\mu_h & 0 & \delta_h & \alpha_h & 0 & 0 & 0 & -k_1 \\ 0 & -m_1 & 0 & 0 & 0 & 0 & 0 & k_1 \\ 0 & q_h & -m_2 & 0 & 0 & 0 & 0 & 0 \\ 0 & 0 & v_h & -m_3 & 0 & 0 & 0 & 0 \\ 0 & 0 & 0 & 0 & h - g & 0 & 0 & 0 \\ 0 & 0 & -k_2 k_3 & 0 & \theta_m c & -\mu_m & 0 & 0 \\ 0 & 0 & k_2 k_3 & 0 & 0 & 0 & -m_4 & 0 \\ 0 & 0 & 0 & 0 & 0 & 0 & q_m & -\mu_m \end{pmatrix} \quad (3.4)$$

where $m_1 = q_h + \mu_h$, $m_2 = \delta_h + \mu_h + v_h$, $m_3 = \alpha_h + \mu_h$, $m_4 = q_m + \mu_m$

FIGURE 3. Contour plot of R_{01} for $\theta_m = 0.7$

The eigenvalues corresponding to equation (3.4) is given by $\lambda_1 = h - g < 0$, $\lambda_2 = -\mu_h$, $\lambda_3 = -(\alpha_h + \mu_h)$, $\lambda_4 = -\mu_m$

The rest four roots can be obtain from the following polynomial

$$P(\lambda) = \lambda^4 + A_0\lambda^3 + A_1\lambda^2 + A_2\lambda + A_3 \quad (3.5)$$

where

$$\begin{aligned} A_0 &= \delta_h + 2\mu_h + q_h + v_h + 2\mu_m + q_m \\ A_1 &= \delta_h\mu_h + \mu_h^2 + 2\delta_h\mu_m + 4\mu_h\mu_m + \delta_hq_m + 2\mu_hq_m + 2q_h\mu_m \\ &\quad + v_hq_m + q_hq_m + 2v_h\mu_m + \delta_hq_h + \mu_hq_h + q_hv_h + \mu_hv_h + \mu_m^2 + \mu_mq_m \\ A_2 &= 2\delta_h\mu_h\mu_m + \delta_h\mu_m^2 + 2\mu_h^2\mu_m + 2\mu_h\mu_m^2 + \delta_h\mu_hq_m \\ &\quad + 2\delta_hq_h\mu_m + \delta_h\mu_mq_m + \delta_hq_hq_m + \mu_h^2q_m + \mu_hq_hq_m + 2\mu_hq_h\mu_m \\ &\quad + 2\mu_h\mu_mq_m + q_h\mu_m^2 + q_hv_hq_m + \mu_hv_hq_m + 2q_hv_h\mu_m + v_h\mu_mq_m + q_hv_hq_m \\ &\quad + 2\mu_hv_h\mu_m + v_h\mu_m^2 \\ A_3 &= -k_1k_2k_3q_m + \delta_h\mu_h\mu_m^2 + \mu_h^2\mu_m^2 + \delta_h\mu_h\mu_mq_m \\ &\quad + \delta_hq_h\mu_m^2 + \delta_hq_h\mu_mq_m + \mu_h^2\mu_mq_m + \mu_hq_h\mu_m^2 + \mu_hq_h\mu_mq_m \\ &\quad + \mu_hv_h\mu_mq_m + q_hv_h\mu_m^2 + q_hv_h\mu_mq_m + \mu_hv_h\mu_m^2 \\ &= \frac{(k_0 - k_1k_2k_3q_m)[\mu_m(q_h + \mu_h)(v_h + \delta_h + \mu_h)(q_m + \mu_m)]}{k_1k_2k_3q_hq_m + (\mu(q_h + \mu_h)(v_h + \delta_h + \mu_h)(q_m + \mu_m))} [R_{01}^2 - 1] \end{aligned}$$

where

$$\begin{aligned} k_0 = & \delta_h \mu_h \mu_m^2 + \mu_h^2 \mu_m^2 + \delta_h \mu_h \mu_m q_m + \delta_h q_h \mu_m^2 \\ & + \delta_h q_h \mu_m q_m + \mu_h^2 \mu_m q_m + \mu_h q_h \mu_m^2 + \mu_h q_h \mu_m q_m \\ & + \mu_h v_h \mu_m q_m + q_h v_h \mu_m^2 + q_h v_h \mu_m q_m + \mu_h v_h \mu_m^2 \end{aligned}$$

□

Remark 1. Clearly, $A_0, A_1, A_2, A_3 > 0$, provided that $R_{01}^2 < 1$ and $\frac{(k_0 - k_1 k_2 k_3 q_m) [\mu_m (q_h + \mu_h) (v_h + \delta_h + \mu_h) (q_m + \mu_m)]}{[k_1 k_2 k_3 q_m + (\mu (q_h + \mu_h) (v_h + \delta_h + \mu_h) (q_m + \mu_m))]} < 0$. Thus, the DFE corresponding to the continuous presence of invasive plants in human environment is locally asymptotically stable (LAS).

3.4. Local asymptotic stability (LAS) of E_2 equilibrium.

Theorem 3.2. For $R_{02}^2 < 1$, E_2 is locally asymptotically stable and unstable if $R_{02}^2 > 1$.

Proof. Linearising the model equations (3.1) with the corresponding equilibrium, E_2 and obtained the following:

$$J(E_2) = \begin{pmatrix} -\mu_h & 0 & \delta_h & \alpha_h & 0 & 0 & 0 & -k_1 \\ 0 & -m_1 & 0 & 0 & 0 & 0 & 0 & k_1 \\ 0 & q_h & -m_2 & 0 & 0 & 0 & 0 & 0 \\ 0 & 0 & v_h & -m_3 & 0 & 0 & 0 & 0 \\ 0 & 0 & 0 & 0 & g - h & 0 & 0 & 0 \\ 0 & 0 & -k_2 & 0 & \theta_m c & -\mu_m & 0 & 0 \\ 0 & 0 & k_2 & 0 & 0 & 0 & -m_4 & 0 \\ 0 & 0 & 0 & 0 & 0 & 0 & q_m & -\mu_m \end{pmatrix} \quad (3.6)$$

where $m_1 = q_h + \mu_h, m_2 = \delta_h + \mu_h + v_h, m_3 = \alpha_h + \mu_h, m_4 = q_m + \mu_m$. The eigenvalues corresponding to equation (3.6) is given by $x_1 = g - h = 0, x_2 = -\mu_h, x_3 = -(\alpha_h + \mu_h), x_4 = -\mu_m$

The rest four roots can be obtain from the following polynomial

$$x^4 + B_0 x^3 + B_1 x^2 + B_2 x + B_3 = 0 \quad (3.7)$$

where

$$\begin{aligned} B_0 &= \delta_h + 2\mu_h + q_h + v_h + 2\mu_m + q_m \\ B_1 &= \delta_h \mu_h + \mu_h^2 + 2\delta_h \mu_m + 4\mu_h \mu_m + \delta_h q_m + 2\mu_h q_m + 2q_h \mu_m \\ &\quad + v_h q_m + q_h q_m + 2v_h \mu_m + \delta_h q_h + \mu_h q_h + q_h v_h + \mu_h v_h + \mu_m^2 + \mu_m q_m \\ B_2 &= 2\delta_h \mu_h \mu_m + \delta_h \mu_m^2 + 2\mu_h^2 \mu_m + 2\mu_h \mu_m^2 + \delta_h \mu_h q_m \\ &\quad + 2\delta_h q_h \mu_m + \delta_h \mu_m q_m + \delta_h q_h q_m + \mu_h^2 q_m + \mu_h q_h q_m + 2\mu_h q_h \mu_m \\ &\quad + 2\mu_h \mu_m q_m + q_h \mu_m^2 + q_h \mu_m q_m + \mu_h v_h q_m + 2q_h v_h \mu_m + v_h \mu_m q_m \\ &\quad + q_h v_h q_m + 2\mu_h v_h \mu_m + v_h \mu_m^2 \\ B_3 &= -k_1 k_2 q_m + \delta_h \mu_h \mu_m^2 + \mu_h^2 \mu_m^2 + \delta_h \mu_h \mu_m q_m + \delta_h q_h \mu_m^2 \\ &\quad + \delta_h q_h \mu_m q_m + \mu_h^2 \mu_m q_m + \mu_h q_h \mu_m^2 + \mu_h q_h \mu_m q_m + \mu_h v_h \mu_m q_m \\ &\quad + q_h v_h \mu_m^2 + q_h v_h \mu_m q_m + \mu_h v_h \mu_m^2 \\ &= \frac{(k_0 - k_1 k_2 q_m) [\mu_m (q_h + \mu_h) (v_h + \delta_h + \mu_h) (q_m + \mu_m)]}{k_1 k_2 q_m + (\mu (q_h + \mu_h) (v_h + \delta_h + \mu_h) (q_m + \mu_m))} [R_{02}^2 - 1] \end{aligned}$$

where

$$\begin{aligned} k_0 = & \delta_h \mu_h \mu_m^2 + \mu_h^2 \mu_m^2 + \delta_h \mu_h \mu_m q_m + \delta_h q_h \mu_m^2 \\ & + \delta_h q_h \mu_m q_m + \mu_h^2 \mu_m q_m + \mu_h q_h \mu_m^2 + \mu_h q_h \mu_m q_m \\ & + \mu_h v_h \mu_m q_m + q_h v_h \mu_m^2 + q_h v_h \mu_m q_m + \mu_h v_h \mu_m^2 \end{aligned}$$

□

3.4.1. *Remark 2.* Clearly, $B_0, B_1, B_2, B_3 > 0$ provided that $R_{02}^2 < 1$ and

$$\frac{(k_0 - k_1 k_2 q_h q_m) [\mu_m (q_h + \mu_h) (v_h + \delta_h + \mu_h) (q_m + \mu_m)]}{[k_1 k_2 q_m + (\mu (q_h + \mu_h) (v_h + \delta_h + \mu_h) (q_m + \mu_m))]} < 0.$$

Since one of the eigenvalues is zero, further analysis using the Center Manifold Theory will have to be used in establishing the LAS of E_2 in the manifold of interest. However, since the other eigenvalues are negative, with the associated effective reproduction number less than unity, we conjecture that E_2 , at most stable, and an attractor of trajectories in its neighbourhood. E_2 is stable but may not be asymptotically stable since this DFE exists only when $g = h$. These results show an important effect of the presence of invasive alien plants on malaria dynamics: they can lead to the existence of two DFEs. This is an important contribution to knowledge.

3.5. Disease endemic equilibrium.

Theorem 3.3. *System (3.1) has a unique positive equilibrium, $E_3 = (S_h^{**}, E_h^{**}, I_h^{**}, R_h^{**}, P^{**}, S_m^{**}, E_m^{**}, I_m^{**})$ whenever $R_{01}^2 > 1$.*

Proof. We will begin the analysis of the disease model endemic equilibrium by rewritten system (3.1) in terms of the force of infections as follows:

$$\begin{aligned} \frac{dS_h}{dt} &= \mu_h (1 - S_h) + \delta_h I_h + \alpha_h R_h - \lambda_h S_h \\ \frac{dE_h}{dt} &= \lambda_h S_h - (q_h + \mu_h) E_h \\ \frac{dI_h}{dt} &= q_h E_h - (\delta_h + \mu_h + v_h) I_h \\ \frac{dR_h}{dt} &= v_h I_h - (\mu_h + \alpha_h) R_h \\ \frac{dP}{dt} &= g(1 - P)P - hP \\ \frac{dS_m}{dt} &= \mu_m (1 - S_m) + \theta_m cP - \lambda_m S_m \\ \frac{dE_m}{dt} &= \lambda_m S_m - (q_m + \mu_m) E_m \\ \frac{dI_m}{dt} &= q_m E_m - \mu_m I_m \end{aligned} \tag{3.8}$$

where

$$\lambda_h = \phi \beta_{hm} \frac{b I_m}{N_h}, \lambda_m = \phi \beta_{mh} \frac{b I_h}{N_h}$$

To obtain this equilibrium, we set the right hand sides of (3.8), and solve for the state variables. After several calculations, we have that

$$E_3 = (S_h^{**}, E_h^{**}, I_h^{**}, R_h^{**}, P^{**}, S_m^{**}, E_m^{**}, I_m^{**})$$

where

$$\begin{aligned}
S_h^{**} &= \frac{\mu_h a_1 a_2 a_3}{(a_1 a_2 a_3 - \delta_h \alpha_h - \delta_h \mu_h - \alpha_h v_h) \lambda_h^{**} + \mu_h a_1 a_2 a_3} \\
E_h^{**} &= \frac{a_2 a_3 \mu_h \lambda_h^{**}}{(a_1 a_2 a_3 - \delta_h \alpha_h - \delta_h \mu_h - \alpha_h v_h) \lambda_h^{**} + \mu_h a_1 a_2 a_3} \\
I_h^{**} &= \frac{\mu_h a_3 q_h \lambda_h^{**}}{(a_1 a_2 a_3 - \delta_h \alpha_h - \delta_h \mu_h - \alpha_h v_h) \lambda_h^{**} + \mu_h a_1 a_2 a_3} \\
R_h^{**} &= \frac{\mu_h v_h q_h \lambda_h^{**}}{(a_1 a_2 a_3 - \delta_h \alpha_h - \delta_h \mu_h - \alpha_h v_h) \lambda_h^{**} + \mu_h a_1 a_2 a_3} \\
P^{**} &= \frac{K_p(g-h)}{g}, g > h \\
S_m^{**} &= \frac{\mu_m g + \theta_m c(g-h)}{g(\mu_m + \lambda_m^{**})}, \\
E_m^{**} &= \frac{\lambda_m^{**}(\mu_m g + \theta_m c(g-h))}{g(\mu_m + \lambda_m^{**})(q_m + \mu_m)}, \\
I_m^{**} &= \frac{\lambda_m^{**}(\mu_m g + \theta_m c(g-h))}{\mu_m g(\mu_m + \lambda_m^{**})(q_m + \mu_m)}, \\
N_h^{**} &= \frac{\mu_h(a_1 a_2 a_3 + \lambda_h^{**}(a_2 a_3 + a_3 q_h + v_h q_h))}{(a_1 a_2 a_3 - \delta_h \alpha_h - \delta_h \mu_h - \alpha_h v_h) \lambda_h^{**} + \mu_h a_1 a_2 a_3}
\end{aligned} \tag{3.9}$$

with

$$a_1 = q_h + \mu_h, a_2 = \delta_h + \mu_h + v_h, a_3 = \mu_h + \alpha_h$$

and

$$\lambda_h^{**} = \phi \beta_{hm} \frac{b I_m^{**}}{N_h^{**}}, \lambda_m^{**} = \phi \beta_{mh} \frac{b I_h^{**}}{N_h^{**}} \tag{3.10}$$

for

$$\phi = (1 - \epsilon \gamma)$$

substituting equations (3.9) in equations (3.10) show that the non-zero equilibrium of the model can be written in a compact form as:

$$Z_1 \lambda_h^{**2} + Z_2 \lambda_h^{**} + Z_3 = 0 \tag{3.11}$$

where

$$\begin{aligned}
Z_1 &= \delta_h [a_3^2 b g \phi \mu_h^2 q_h^2 \mu_m^2 \beta_{mh} + a_2 a_3^2 b g \phi \mu_h^2 q_h \mu_m^2 \beta_{mh} + a_3^2 b g \phi \mu_h^2 q_h^2 \mu_m q_m \beta_{mh} \\
&\quad + a_2 a_3^2 b g \phi \mu_h^2 q_h \mu_m q_m \beta_{mh} + a_3 b g \phi \mu_h^2 q_h^2 v_h \mu_m^2 \beta_{mh} + a_3 b g \phi \mu_h^2 q_h^2 v_h \mu_m q_m \beta_{mh} \\
&\quad + a_1 a_2 a_3^2 g \mu_h^2 \mu_m^3 + a_3^2 g \mu_h^2 q_h^2 \mu_m^3 + a_1 a_3^2 g \mu_h^2 q_h \mu_m^3 + a_2 a_3^2 g \mu_h^2 q_h \mu_m^3 + a_1 a_2 a_3^2 g \mu_h^2 \mu_m^2 q_m + a_3^2 g \mu_h^2 q_h^2 \mu_m^2 q_m \\
&\quad + a_1 a_3^2 g \mu_h^2 q_h \mu_m^2 q_m + a_2 a_3^2 g \mu_h^2 q_h \mu_m^2 q_m + 2 a_3 g \mu_h^2 q_h^2 v_h \mu_m^3 + a_1 a_3 g \mu_h^2 q_h v_h \mu_m^3 + a_2 a_3 g \mu_h^2 q_h v_h \mu_m^3 \\
&\quad + 2 a_3 g \mu_h^2 q_h^2 v_h \mu_m^2 q_m + a_1 a_3 g \mu_h^2 q_h v_h \mu_m^2 q_m + a_2 a_3 g \mu_h^2 q_h v_h \mu_m^2 q_m + g \mu_h^2 q_h^2 v_h^2 \mu_m^3 + g \mu_h^2 q_h^2 v_h^2 \mu_m^2 q_m]
\end{aligned}$$

$$\begin{aligned}
Z_2 = & a_3 b^2 c g \phi^2 \alpha_h \delta_h \mu_h q_h \beta_{hm} \theta_m q_m \beta_{mh} + a_3 b^2 c g \phi^2 \delta_h \mu_h^2 q_h \beta_{hm} \theta_m q_m \beta_{mh} \\
& - a_1 a_2 a_3^2 b^2 c g \phi^2 \mu_h q_h \beta_{hm} \theta_m q_m \beta_{mh} + a_3 b^2 c g \phi^2 \alpha_h \mu_h q_h v_h \beta_{hm} \theta_m q_m \beta_{mh} \\
& - a_3 b^2 c h \phi^2 \alpha_h \delta_h \mu_h q_h \beta_{hm} \theta_m q_m \beta_{mh} - a_3 b^2 c h \phi^2 \delta_h \mu_h^2 q_h \beta_{hm} \theta_m q_m \beta_{mh} + a_1 a_2 a_3^2 b^2 c h \phi^2 \mu_h q_h \beta_{hm} \theta_m q_m \beta_{mh} \\
& - a_3 b^2 c h \phi^2 \alpha_h \mu_h q_h v_h \beta_{hm} \theta_m q_m \beta_{mh} + a_3 b^2 g \phi^2 \alpha_h \delta_h \mu_h q_h \beta_{hm} \mu_m q_m \beta_{mh} + a_3 b^2 g \phi^2 \delta_h \mu_h^2 q_h \beta_{hm} \mu_m q_m \beta_{mh} \\
& - a_1 a_2 a_3^2 b^2 g \phi^2 \mu_h q_h \beta_{hm} \mu_m q_m \beta_{mh} + a_3 b^2 g \phi^2 \alpha_h \mu_h q_h v_h \beta_{hm} \mu_m q_m \beta_{mh} + a_1 a_2 a_3^2 b g \phi \mu_h^2 q_h \mu_m^2 \beta_{mh} \\
& + a_1 a_2 a_3^2 b g \phi \mu_h^2 q_h \mu_m q_m \beta_{mh} + a_1 a_2^2 a_3^2 g \mu_h^2 \mu_m^3 + a_1^2 a_2 a_3^2 g \mu_h^2 \mu_m^3 + 2 a_1 a_2 a_3^2 g \mu_h^2 q_h \mu_m^3 + a_1 a_2^2 a_3^2 g \mu_h^2 \mu_m^2 q_m \\
& + a_1^2 a_2 a_3^2 g \mu_h^2 \mu_m^2 q_m + 2 a_1 a_2 a_3^2 g \mu_h^2 q_h \mu_m^2 q_m + 2 a_1 a_2 a_3 g \mu_h^2 q_h v_h \mu_m^3 + 2 a_1 a_2 a_3 g \mu_h^2 q_h v_h \mu_m^2 q_m \\
Z_3 = & -a_1 a_2 a_3^2 b^2 c g \phi^2 \mu_h^2 q_h \beta_{hm} \theta_m q_m \beta_{mh} + a_1 a_2 a_3^2 b^2 c h \phi^2 \mu_h^2 q_h \beta_{hm} \theta_m q_m \beta_{mh} \\
& - a_1 a_2 a_3^2 b^2 g \phi^2 \mu_h^2 q_h \beta_{hm} \mu_m q_m \beta_{mh} + a_1^2 a_2^2 a_3^2 g \mu_h^2 \mu_m^3 + a_1^2 a_2^2 a_3^2 g \mu_h^2 \mu_m^2 q_m \\
= & \frac{a_1 a_2 \mu_m (a_1 a_2 a_3^2 b^2 c h \phi^2 \mu_h^2 q_h \beta_{hm} \theta_m q_m \beta_{mh} + a_1^2 a_2^2 a_3^2 g \mu_h^2 \mu_m^2 q_m - \tau)(q_m + \mu_m)}{a_1 a_2 \mu_m (q_m + \mu_m) + k_1 k_2 k_3 q_m} [1 - R_{01}^2]
\end{aligned}$$

where

$$\tau = a_1 a_2 a_3^2 b^2 c g \phi^2 \mu_h^2 q_h \beta_{hm} \theta_m q_m \beta_{mh} + a_1 a_2 a_3^2 b^2 g \phi^2 \mu_h^2 q_h \beta_{hm} \mu_m q_m \beta_{mh}$$

There are three cases to be considered (depending on the signs of Z_1 and Z_3 , since Z_1 is positive) to study the number of positive roots of $f(\lambda_h^{**}) = 0$.

- **Case 1:** Suppose $\delta_h = 0$ then $Z_1 = 0$, $Z_2 > 0$ and the quadratic equation (3.11) becomes linear in $\lambda_h^{**} = \frac{-Z_3}{Z_2}$. Hence, there will be a unique positive root if $Z_3 < 0$. In this case, the system has a unique (stable) endemic equilibrium if and only if $Z_3 < 0$ which occurs only when $R_{01}^2 > 1$; hence backward bifurcation is not possible in this case.
- **Case 2:** If $Z_2 < 0$ and $Z_3 = 0$ or $Z_2^2 - 4Z_1Z_3 = 0$, then $f(\lambda_h^{**}) = 0$ has one positive root which means that the system has a unique endemic equilibrium.
- **Case 3:** If $Z_3 > 0$ and $Z_2 < 0$ or $Z_2^2 - 4Z_1Z_3 > 0$, then $f(\lambda_h^{**}) = 0$ has two positive roots which implies that the system has two equilibria.

We therefore summarized the results in the following lemma. □

Lemma 1. The number of positive endemic equilibria of model (3.11) is summarized as follows:

- (1) If $Z_3 < 0 \Leftrightarrow R_{01}^2 > 1$, the system has a unique endemic equilibrium.
- (2) If $Z_2 < 0$ and $Z_3 = 0$ or $Z_2^2 - 4Z_1Z_3 = 0$, the system has exactly one endemic equilibrium.
- (3) If $Z_3 > 0 \Leftrightarrow R_{01}^2 < 1$ and $Z_2^2 - 4Z_1Z_3 > 0$, the system has exactly two endemic equilibria.
- (4) Otherwise there are no endemic equilibria, i.e. when $Z_1Z_3 > 0$ and $Z_2 > 0$,

where $g > h$.

3.6. Backward bifurcation phenomenon. Backward bifurcation may occur under certain conditions for $R_{01}^2 < 1$. The presence of backward bifurcation indicates that the necessary requirement of $R_{01}^2 < 1$, is not sufficient for the disease elimination. The Center Manifold Theory will be used to prove the conditions on existence of backward bifurcation. To investigate the existence of the backward bifurcation of the spatially homogeneous

of model (3.1), we shall rewrite it in vector form as:

$$\frac{dY}{dt} = H(y) \quad (3.12)$$

where

$$Y = (y_1, y_2, y_3, y_4, y_5, y_6, y_7, y_8)^T$$

and

$$H = (h_1, h_2, h_3, h_4, h_5, h_6, h_7, h_8)^T$$

so that

$$S_h = y_1, E_h = y_2, I_h = y_3, R_h = y_4, P = y_5, S_m = y_6, E_m = y_7, I_m = y_8$$

Thus, it becomes

$$\begin{aligned} \dot{y}_1 &= h_1 = \mu_h(1 - y_1) + \delta_h y_3 + \alpha_h y_4 - (1 - \epsilon\gamma)\beta_{hm} b y_1 y_8 \\ \dot{y}_2 &= h_2 = (1 - \epsilon\gamma)\beta_{hm} b y_1 y_8 - (q_h + \mu_h)y_2 \\ \dot{y}_3 &= h_3 = q_h y_2 - (\delta_h + \mu_h + v_h)y_3 \\ \dot{y}_4 &= h_4 = v_h y_3 - (\mu_h + \alpha_h)y_4 \\ \dot{y}_5 &= h_5 = g(1 - y_5)y_5 - h y_5 \\ \dot{y}_6 &= h_6 = \mu_m(1 - y_6) + \theta_m c y_5 - (1 - \epsilon\gamma) b x y_3 y_6 \\ \dot{y}_7 &= h_7 = (1 - \epsilon\gamma) b x y_3 y_6 - (q_m + \mu_m)y_7 \\ \dot{y}_8 &= h_8 = q_m y_7 - \mu_m y_8 \end{aligned} \quad (3.13)$$

Theorem 3.4. For $\beta_{mh} = \beta_{mh}^* = \sqrt{\frac{k_1 k_2 k_3 q_m (q_m + \mu_m)}{\mu_m (q_h + \mu_h) (v_h + \delta_h + \mu_h) (q_m + \mu_m) (q_m + \mu_m)}}$ then system (3.1) exhibits a backward bifurcation phenomenon whenever $a, b > 0$.

Proof. Choosing β_{mh} as the bifurcation parameter at $R_{01}^2 = 1$, We have

$$\beta_{mh} = \beta_{mh}^* = \sqrt{\frac{k_1 k_2 k_3 q_m (q_m + \mu_m)}{\mu_m (q_h + \mu_h) (v_h + \delta_h + \mu_h) (q_m + \mu_m) (q_m + \mu_m)}} \quad (3.14)$$

$$J(E_1, \beta_{mh}^*) = \begin{pmatrix} -\mu_h & 0 & 0 & \alpha_h & 0 & 0 & 0 & -k_1 \\ 0 & -m_5 & 0 & 0 & 0 & 0 & 0 & k_1 \\ 0 & q_h & -m_6 & 0 & 0 & 0 & 0 & 0 \\ 0 & 0 & v_h & -m_7 & 0 & 0 & 0 & 0 \\ 0 & 0 & 0 & 0 & h - g & 0 & 0 & 0 \\ 0 & 0 & -k_2 k_3 & 0 & \theta_m c & -\mu_m & 0 & 0 \\ 0 & 0 & k_2 k_3 & 0 & 0 & 0 & -m_8 & 0 \\ 0 & 0 & 0 & 0 & 0 & 0 & q_m & -\mu_m \end{pmatrix} \quad (3.15)$$

where $m_5 = q_h + \mu_h, m_6 = \delta_h + \mu_h + v_h, m_7 = \alpha_h + \mu, m_8 = q_m + \mu_m$

Thus, the right eigenvector, $w = (w_1, w_2, w_3, w_4, w_5, w_6, w_7, w_8)^T$, associated with the simple zero eigenvalue can be obtained from $J(E_1, \beta_{mh}^*) \cdot w = 0$. Thus, we get

$$\begin{aligned} w_1 &= \frac{\delta_h w_3 + \alpha_h w_4 - k_1 w_8}{\mu_h}, w_2 = \frac{k_1 w_8}{q_h + \mu_h}, \\ w_3 &= \frac{q_h w_2}{\delta_h + v_h + \mu_h}, w_4 = \frac{v_h w_3}{\alpha_h + \mu_h}, \\ w_5 &= 0, w_6 = -\frac{k_2 k_3 w_3}{\mu_h}, w_7 = -\frac{k_2 k_3 w_3}{q_m + \mu_m}, w_8 = \frac{q_m w_7}{\mu_m} \end{aligned} \quad (3.16)$$

More so, the left eigenvector, $v = (v_1, v_2, \dots, v_8)$, corresponding to the simple zero eigenvalues is obtained from $v \cdot J(E_1, \beta_{mh}^*) = 0$. Thus,

$$\begin{aligned} v_1 = 0, v_2 = \frac{q_h v_3}{q_h + \mu_h}, v_3 = v_3 > 0, v_4 = 0, \\ v_5 = 0, v_6 = 0, v_7 = \frac{q_m v_8}{q_m + \mu_m}, v_8 = \frac{k_1 v_2}{\mu_m} \end{aligned} \quad (3.17)$$

□

Therefore, the second-order partial derivatives of h_i , $i = 1, 2, \dots, 8$ from system (3.13) are zero at point (E_1, β_{mh}^*) except the following.

$$\begin{aligned} \frac{\partial^2 h_1}{\partial y_1 \partial y_8} &= -(1 - \epsilon\gamma)\beta_{hm}^* b, \quad \frac{\partial^2 h_2}{\partial y_1 \partial y_8} = (1 - \epsilon\gamma)\beta_{hm}^* b \\ \frac{\partial^2 h_5}{\partial y_5 \partial y_5} &= -2g, \quad \frac{\partial^2 h_6}{\partial y_3 \partial y_6} = -(1 - \epsilon\gamma)\beta_{mh}^* b \\ \frac{\partial^2 h_7}{\partial y_3 \partial y_6} &= (1 - \epsilon\gamma)\beta_{mh}^* b \\ \frac{\partial^2 h_1}{\partial y_8 \partial \beta_{hm}^*} &= -(1 - \epsilon\gamma)b, \quad \frac{\partial^2 h_2}{\partial y_8 \partial \beta_{hm}^*} = (1 - \epsilon\gamma)b \\ \frac{\partial^2 h_6}{\partial y_3 \partial \beta_{mh}^*} &= -\frac{(1 - \epsilon\gamma)b(\mu_m g + \theta_m c(g - h))}{\mu_m g} \\ \frac{\partial^2 h_7}{\partial y_3 \partial \beta_{mh}^*} &= \frac{(1 - \epsilon\gamma)b(\mu_m g + \theta_m c(g - h))}{\mu_m g} \end{aligned} \quad (3.18)$$

Assuming that

- (1) $\mathbf{A} = D_x h(0, 0) = (\frac{\partial h_i}{\partial x_j}, 0, 0)$ is the linearized matrix of the system around the equilibrium 0 with σ evaluated at 0. Zero is a simple eigenvalue of \mathbf{A} and all other eigenvalues of \mathbf{A} have negative real parts;
- (2) Matrix \mathbf{A} have a non-negative right eigenvector, w and a left eigenvector, v corresponding to the zero eigenvalue. Let h_k be the k -th component of h and

$$\begin{aligned} a &= \sum_{k,i,j=1}^n v_k w_i w_j \frac{\partial^2 h_k}{\partial y_i \partial y_j}(0, 0), \\ b &= \sum_{k,i=1}^n v_k w_i \frac{\partial^2 h_k}{\partial y_i \partial \sigma}(0, 0). \end{aligned} \quad (3.19)$$

The local dynamics of system (3.13) around 0 are totally determined by a and b . By virtue of the Center Manifold Theory (Castillo and Song, 2014), we calculated the bifurcation

parameter to be

$$\begin{aligned}
 a &= v_1 \sum_{i,j=1}^8 w_i w_j \frac{\partial^2 h_1}{\partial y_i \partial y_j} + v_2 \sum_{i,j=1}^8 w_i w_j \frac{\partial^2 h_2}{\partial y_i \partial y_j} \\
 &+ v_5 \sum_{i,j=1}^8 w_i w_j \frac{\partial^2 h_5}{\partial y_i \partial y_j} + v_6 \sum_{i=1}^8 w_i w_j \frac{\partial^2 h_6}{\partial y_i \partial y_j} \\
 &+ v_7 \sum_{i,j=1}^8 w_i w_j \frac{\partial^2 h_7}{\partial y_i \partial y_j} \\
 &= (1 - \epsilon\gamma)\beta_{hm}^* b v_2 + (1 - \epsilon\gamma)\beta_{mh}^* b v_7 > 0.
 \end{aligned} \tag{3.20}$$

Also,

$$\begin{aligned}
 b &= v_1 \sum_{i=1}^8 w_i \frac{\partial^2 h_1}{\partial y_i \partial \beta_{hm}^*} + v_2 \sum_{i=1}^8 w_i \frac{\partial^2 h_2}{\partial y_i \partial \beta_{hm}^*} \\
 &+ v_6 \sum_{i=1}^8 w_i \frac{\partial^2 h_6}{\partial y_i \partial \beta_{mh}^*} + v_7 \sum_{i=1}^8 w_i \frac{\partial^2 h_7}{\partial y_i \partial \beta_{mh}^*} \\
 &= (1 - \epsilon\gamma) b v_2 + \frac{(1 - \epsilon\gamma) b (\mu_m g + \theta_m c (g - h)) v_7}{\mu_m g} > 0.
 \end{aligned} \tag{3.21}$$

We therefore conclude that a backward bifurcation occurs since $a > 0$ and $b > 0$.

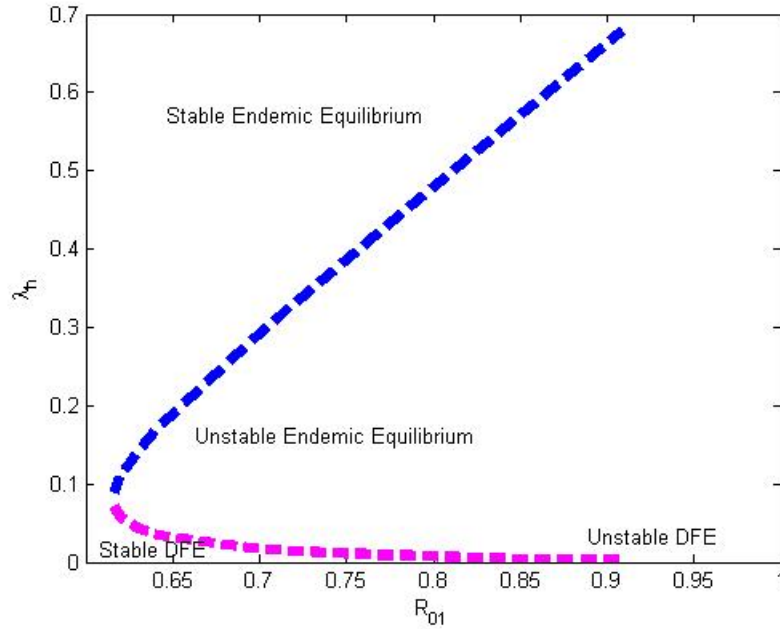


FIGURE 4. Bifurcation diagram of System (3)

3.7. Global stability of the endemic equilibrium. The global asymptotic stability of the endemic equilibrium (E_3) of the spatial homogeneous model (3.1) will now be investigated. We defined the following set.

$$\Omega = \{(S_h, E_h, I_h, R_h, P, S_m, E_m, I_m) \in C([0]), R_+^8, T_0; 0 < S_h < S_h^{**}, E_h(t) \leq E_h^{**}, I_h(t) \leq I_h^{**}, R_h(t) \leq R_h^{**}, P(t) \leq P^{**}, S_m(t) \leq S_m^{**}, E_m(t) \leq E_m^{**}, I_m(t) \leq I_m^{**}\}$$

since $\Omega \in C([0], R_+^8)$, it follows that Ω is positively invariant with respect to the special case of the spatial homogeneous model (3.1) mention above. The following theorem holds

Theorem 3.5. *The endemic equilibrium (E_3) of the spatial homogeneous model (3.1) with $\delta_h = 0$ is GAS in Ω whenever $R_{01} > 1$.*

Proof. Consider the special case of the spatial homogeneous model with $\delta_h = 0$ and $R_{01} > 1$. Let $E_3 = (S_h^{**}, E_h^{**}, I_h^{**}, R_h^{**}, P^{**}, S_m^{**}, E_m^{**}, I_m^{**})$ represents the unique endemic equilibrium. Considering the non-Linear Lyapunov function of Goh-volterra type. We obtain

$$V = S_h - S_h^{**} \ln S_h + E_h - E_h^{**} \ln E_h + \frac{d_1}{q_h} (I_h - I_h^{**} \ln I_h) + \frac{d_1 \bar{d}_2}{v_h q_h} (R_h - R_h^{**} \ln R_h) + P - P^{**} \ln P + S_m - S_m^{**} \ln S_m + E_m - E_m^{**} \ln E_m + \frac{d_5}{q_m} (I_m - I_m^{**} \ln I_m)$$

where $\bar{d}_2 = V_h + \mu_h$.

We define the following steady state relations obtained from the spatial homogeneous model (3.1) at the endemic steady state E_1 .

$$\begin{aligned} \mu_h + \alpha_h R_h^{**} &= \lambda_h^{**} S_h^{**} + \mu_h S_h \\ d_1 E_h^{**} &= \lambda_h^{**} S_h^{**} \\ \bar{d}_2 I_h^{**} &= q_h E_h^{**} \\ d_3 R_h^{**} &= V_h I_h^{**} \\ d_4 P^{**} &= g(1 - P^{**})P^{**} - hP^{**}\mu_m\theta_m P^{**} = \lambda_m^{**} S_m^{**} + \mu_m S_m^{**} \\ d_5 E_m^{**} &= \lambda_m^{**} S_m^{**} \\ \mu_m I_m^{**} &= q_m E_m^{**} \end{aligned}$$

The Lyapunov derivative of V is given as

$$\begin{aligned} \dot{V} &= (1 - \frac{S_h^{**}}{S_h})(\mu_h(1 - S_h) + \alpha_h R_h - \lambda_h S_h) \\ &+ (1 - \frac{E_h^{**}}{E_h})(\lambda_h S_h - d_1 E_h) + \frac{d_1}{q_h}(1 - \frac{I_h^{**}}{I_h})(q_h E_h - \bar{d}_2 I_h) \\ &+ \frac{d_1}{\bar{d}_2} v_h q_h (1 - \frac{R_h^{**}}{R_h})(V_h I_h - d_3 R_h) \\ &+ (1 - \frac{P^{**}}{P})(g(1 - P^{**})P - hP) + (1 - \frac{S_m^{**}}{S_m})((1 - S_m)\mu_m + \theta_m P - \lambda_m S_m) \\ &+ (1 - \frac{E_m^{**}}{E_m})(\lambda_m S_m - d_5 E_m) + \frac{d_5}{q_m}((1 - \frac{I_m^{**}}{I_m})(q_m E_m - \mu_m I_m) \end{aligned} \quad (3.22)$$

Using the steady state relations gives the following in Ω and noting that the state variables of the spatial homogeneous model (3.1) are bounded by the values of their endemic steady

state in Ω .

$$\begin{aligned}
\dot{V} = & \mu_h S_h^{**} \left[2 - \frac{S_h^{**}}{S_h} - \frac{S_h}{S_h^{**}} \right] \\
& + d_1 E_h^* \left[5 - \frac{S_h^{**}}{S_h} - \frac{E_h^{**} S_h}{E_h S_h^{**}} - \frac{I_h^{**} E_h}{I_h E_h^{**}} - \frac{R_h^{**} I_h}{R_h I_h^{**}} - \frac{R_h}{R_h^{**}} \right] \\
& + d_4 P^{**} \left[2 - \frac{P^{**}}{P} - \frac{P}{P^{**}} + \mu_m S_m^{**} \left[2 - \frac{S_m^{**}}{S_m} - \frac{S_m}{S_m^{**}} \right] \right. \\
& \left. + d_5 E_m^{**} \left[4 - \frac{S_m^{**}}{S_m} - \frac{E_m^{**} S_m}{E_m S_m^{**}} - \frac{I_m^{**} E_m}{I_m I_m^{**}} - \frac{I_m}{I_m^{**}} \right] \right]
\end{aligned} \tag{3.23}$$

Finally, since the arithmetic mean exceeds the geometric mean, the following inequalities hold.

$$\begin{aligned}
\left[2 - \frac{S_h^{**}}{S_h} - \frac{S_h}{S_h^{**}} \right] & \leq 0 \\
\left[5 - \frac{S_h^{**}}{S_h} - \frac{E_h^{**} S_h}{E_h S_h^{**}} - \frac{I_h^{**} E_h}{I_h E_h^{**}} - \frac{R_h^{**} I_h}{R_h I_h^{**}} - \frac{R_h}{R_h^{**}} \right] & \leq 0 \\
\left[2 - \frac{P^{**}}{P} - \frac{P}{P^{**}} \right] & \leq 0 \\
\left[2 - \frac{S_m^{**}}{S_m} - \frac{S_m}{S_m^{**}} \right] & \leq 0 \\
\left[4 - \frac{S_m^{**}}{S_m} - \frac{E_m^{**} S_m}{E_m S_m^{**}} - \frac{I_m^{**} E_m}{I_m I_m^{**}} - \frac{I_m}{I_m^{**}} \right] & \leq 0
\end{aligned}$$

Thus, we have that $\dot{V} \leq 0$ for $R_{01} > 1$. Hence, \dot{V} is a Lyapunov function in Ω whenever $R_{01} > 1$. Therefore, E_3 is GAS in Ω whenever $R_{01} > 1$. \square

4. NUMERICAL SIMULATION

In this section, we present numerical parameters' values of the formulated model as shown in Table 2.

5. TRAVELLING WAVE SOLUTION

In this section, we shall assess the spatial spread of malaria disease with spatial dispersion of vectors. With this regard, we shall find the travelling wave linking the equilibrium points and determine the conditions for the existence of the propagation speed of such wave. In our model, we assumed that the vector population takes both advection movement (K), which increases the wave speed, and dispersal coefficient D , which depends on the wave propagation speed, v .

Travelling wave solution with respect to our model equation are of the form:
 $E_h(x, t) = e_h(z)$, $I_h(x, t) = i_h(z)$, $R_h(x, t) = r_h(z)$, $E_m(x, t) = e_m(z)$, $I_m(x, t) = i_m(z)$, where $z = x - vt$ and v is the constant wave speed, which we will determine. Replacing the non-homogeneous spatial system (2.4) in wave equation form, we obtain the

TABLE 2. Description of the model parameters' values

Parameter	Value	Reference
Λ_h	47.8980/day	Kenya National Bureau of Statistics
μ_h	0.00004643/day	Kenya National Bureau of Statistics
β_{hm}	0.24/day	(Okuneye and Gumel 2015)
β_{mh}	0.14/day	(Okuneye and Gumel 2015)
q_h	0.083/day	(Okuneye and Gumel 2015)
α_h	0.000017/day	(Augusto et al. 2015)
v_h	0.00265/day	(Okuneye and Gumel 2015)
K_p	40000	Assumed
ϵ	0.5	Variable
γ	0.6	Variable
δ_h	0.0003454/day	(Augusto et al. 2015)
b	0.5	Variable
Λ_m	4700.8980/day	(Kroeger et al. 2013)
θ_m	0.343/day	(Okuneye and Gumel 2015)
q_m	0.091	(Augusto et al. 2015)
g	1.84	(Okuneye and Gumel 2015)
μ_m	0.1041	(Nwankwo and Okuonghae 2019)
ξ_m	0.4	Variable
h	0.05	Variable

following system of ordinary differential equations:

$$\begin{aligned}
 e' + \frac{c_1}{v}(1 - e_h - i_h - r_h)i_m - \frac{(q_h + \mu_h)}{v}e_h &= 0 \\
 i' + \frac{q_h}{v}e_h - \frac{(\delta_h + \mu_h + v_h)}{v}i_h &= 0 \\
 r' + \frac{v_h}{v}i_h - \frac{(\mu_h + \alpha_h)}{v}r_h &= 0 \\
 De_m'' - (k - v)e_m' - \frac{c_2}{v}(1 - e_m - i_m)i_h + (q_m + \mu_m)e_m &= 0 \\
 Di_m'' - (k - v)i_m' - q_me_m - \mu_mi_m &= 0
 \end{aligned} \tag{5.1}$$

where $c_1 = \phi\beta_{hm}b$, $c_2 = \phi\beta_{mh}b$ and $\phi = 1 - \epsilon\gamma$.

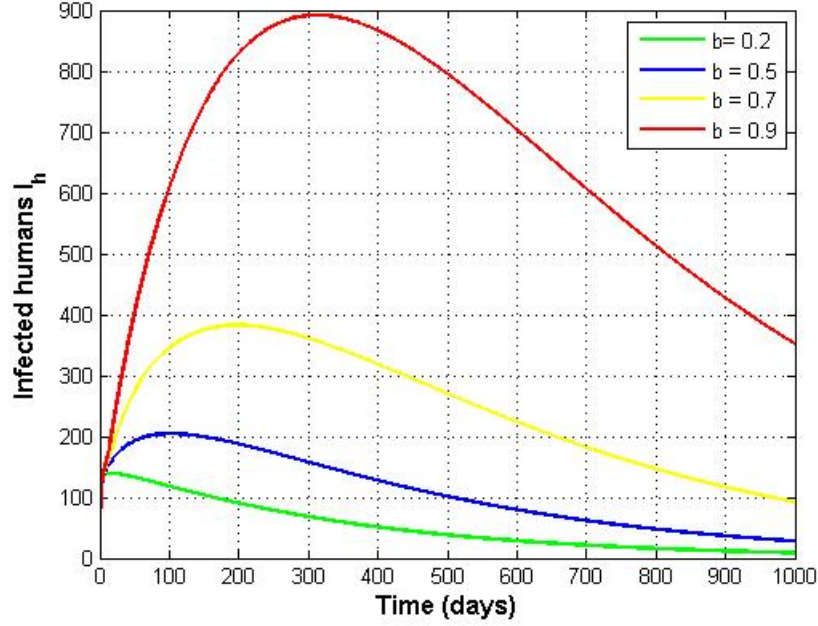


FIGURE 5. Time versus infected human

This system is equivalent to the following system of first-order differential equations:

$$\begin{aligned}
 \frac{de_h}{dz} &= -\frac{c_1}{v}(1 - e_h - i_h - r_h)i_m + \frac{(q_h + \mu_h)}{v}e_h + \frac{\delta_h + v_h + \mu_h}{v}i_h \\
 \frac{di_h}{dz} &= -\frac{q_h}{v}e_h + \frac{(\delta_h + v_h + \mu_h)}{v}i_h \\
 \frac{r_h}{dz} &= \frac{v_h}{v}i_h + \frac{(\alpha_h + \mu_h)}{v}r_h \\
 \frac{e_m}{dz} &= u_1 \\
 \frac{du_1}{dz} &= \frac{1}{D}(k - v)u_1 - \frac{c_2(1 - e_m - i_m)}{D}i_h + \frac{(q_m + \mu_m)}{D}e_m \\
 \frac{di_m}{dz} &= u_2 \\
 \frac{du_2}{dz} &= \frac{1}{D}(k - v)u_2 - \frac{q_m}{D}e_m + \frac{\mu_m}{D}i_m
 \end{aligned} \tag{5.2}$$

where

$$\frac{di_m}{dt} = i_m''(z), \quad \frac{de_m}{dt} = e_m''(z)$$

There are two equilibrium point of the system above the first is $g_1 = (0, 0, 0, 0, 0, 0, 0)$ Which represents disease free equilibrium and the second, $g_2 = (E_h^o, I_h^o, R_h^o, E_m^o, I_m^o, 0, 0)$ which is the non-trivial equilibrium that corresponds to infection the condition for the existence of g_2 is $R_{02} > 1$ because $E_h^o, I_h^o, R_h^o, E_m^o, I_m^o$ are non-negative. We want to find the condition for a solution with a positive wave propagation speed v and with non-negative

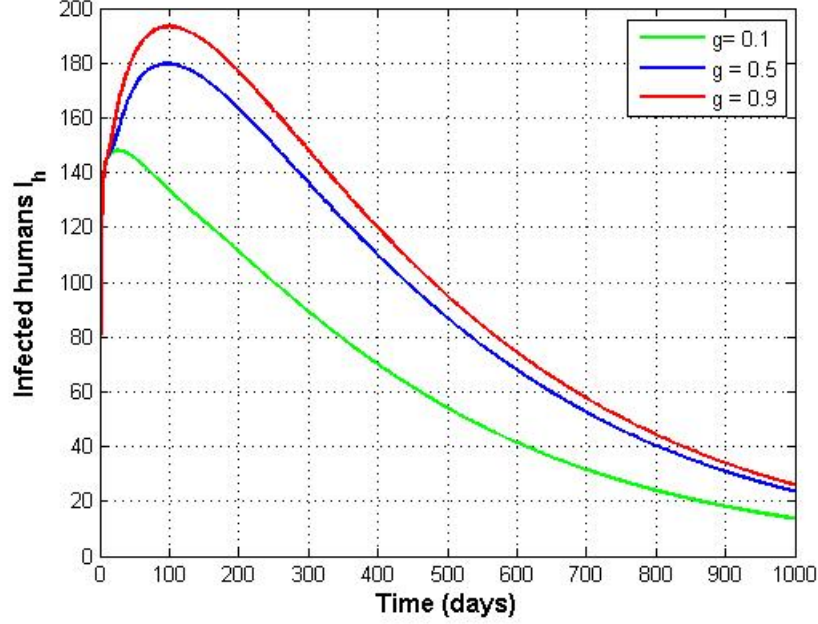


FIGURE 6. Time versus infected human

$E_h^o, I_h^o, R_h^o, E_m^o, I_m^o$ that the following boundary conditions holds.

$$\begin{aligned}
 e_h(-\infty) &= E_h^{**} \quad \text{and} \quad e_h(+\infty) = 0 \\
 i_h(-\infty) &= I_h^{**} \quad \text{and} \quad i_h(+\infty) = 0 \\
 r_h(-\infty) &= R_h^{**} \quad \text{and} \quad r_h(+\infty) = 0 \\
 e_m(-\infty) &= E_m^{**} \quad \text{and} \quad e_m(+\infty) = 0 \\
 i_m(-\infty) &= I_m^{**} \quad \text{and} \quad i_m(+\infty) = 0 \\
 u_1(-\infty) &= 0 \quad \text{and} \quad u_1(+\infty) = 0 \\
 u_2(-\infty) &= 0 \quad \text{and} \quad u_2(+\infty) = 0
 \end{aligned}$$

we searched for solutions in the positive region, such that $E_h^o > 0, I_h^o > 0, R_h^o > 0, E_m^o > 0, I_m^o > 0$ and the solution cannot oscillate near the origin. The eigenvalue of the Jacobian matrix must be real and non complex values otherwise $E_h^o < 0, I_h^o < 0, R_h^o < 0, E_m^o < 0, I_m^o < 0$ for some z . Linearising system (5.2) at point $g_1 = (0, 0, 0, 0, 0, 0, 0)$, we get the Jacobian matrix of the system at g_1 given by

$$Dg_1 = \begin{pmatrix} \frac{q_h + \mu_h}{v} & 0 & 0 & 0 & 0 & -\frac{c_1}{v} & 0 \\ -\frac{q_h}{v} & \frac{\delta_h + v_h + \mu_h}{v} & 0 & 0 & 0 & 0 & 0 \\ 0 & -\frac{v_h}{v} & \frac{\alpha_h + \mu_h}{v} & 0 & 0 & 0 & 0 \\ 0 & 0 & 0 & 0 & 1 & 0 & 0 \\ 0 & -\frac{c_2}{D} & 0 & \frac{q_m + \mu_m}{D} & \frac{k-v}{D} & 0 & 0 \\ 0 & 0 & 0 & 0 & 0 & 0 & 1 \\ 0 & 0 & 0 & -\frac{q_m}{D} & 0 & \frac{\mu_m}{D} & \frac{k-v}{D} \end{pmatrix}, \quad (5.3)$$

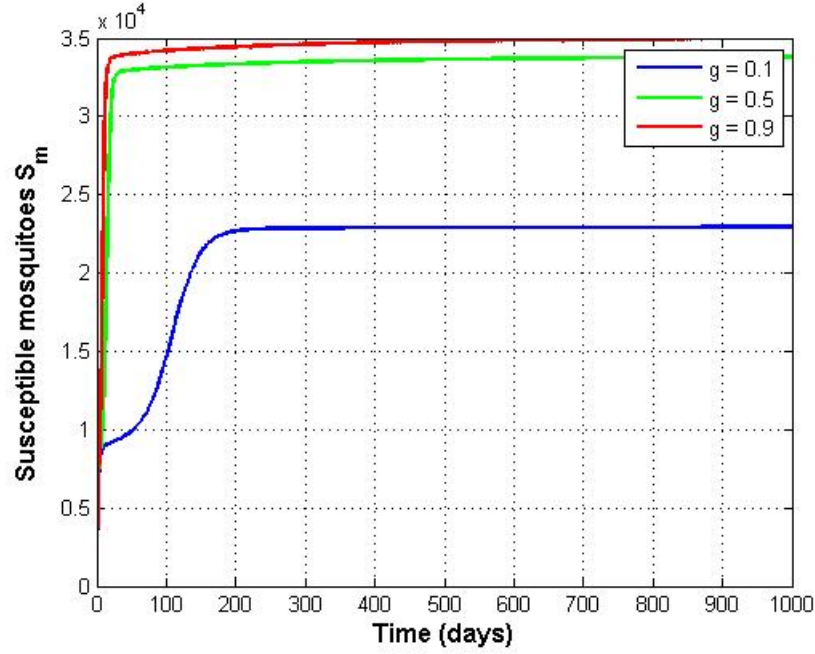


FIGURE 7. Time versus susceptible mosquito

The corresponding eigenvalues of the wave equations are the roots of the polynomial

$$m(\Psi) = \Psi^7 + b_0\Psi^6 + b_1\Psi^5 + b_2\Psi^4 + b_3\Psi^3 + b_4\Psi^2 + b_5\Psi + b_6 \quad (5.4)$$

where

$$b_0 = P_1 + P_2 + P_3 + P_5 + P_6$$

$$b_1 = -\left(\frac{\mu_m}{D} - P_1P_2 - P_3P_2 - P_5P_2 - P_6P_2 - P_1P_3 + P_4 - P_1P_5 - P_3P_5 - P_1P_6 - P_3P_6 - P_5P_6\right)$$

$$b_2 = -\left(\frac{P_3\mu_m}{D} - \frac{P_1\mu_m}{D} - \frac{P_2\mu_m}{D} - \frac{P_5\mu_m}{D} + P_1P_2P_3 - P_4P_3 + P_1P_5P_3 + P_2P_5P_3 + P_1P_6P_3 + P_2P_6P_3 + P_5P_6P_3 - P_1P_4 - P_2P_4 + P_1P_2P_5 + P_1P_2P_6 - P_4P_6 + P_1P_5P_6 + P_2P_5P_6\right)$$

$$b_3 = -\left(-\frac{P_4\mu_m}{D} + \frac{P_1P_2\mu_m}{D} + \frac{P_1P_3\mu_m}{D} + \frac{P_2P_3\mu_m}{D} + \frac{P_1P_5\mu_m}{D} + \frac{P_2P_5\mu_m}{D} + \frac{P_3P_5\mu_m}{D} + P_1P_2P_4 + P_1P_3P_4 + P_2P_3P_4 + P_1P_6P_4 + P_2P_6P_4 + P_3P_6P_4 - P_1P_2P_3P_5 - P_1P_2P_3P_6 - P_1P_2P_5P_6 - P_1P_3P_5P_6 - P_2P_3P_5P_6\right)$$

$$b_4 = -\left(\frac{P_1P_4\mu_m}{D} + \frac{P_2P_4\mu_m}{D} + \frac{P_3P_4\mu_m}{D} - \frac{P_1P_2P_3\mu_m}{D} - \frac{P_1P_2P_5\mu_m}{D} - \frac{P_1P_3P_5\mu_m}{D} - \frac{P_2P_3P_5\mu_m}{D} - P_1P_2P_3P_4 - P_1P_2P_6P_4 - P_1P_3P_6P_4 - P_2P_3P_6P_4 + P_1P_2P_3P_5P_6\right)$$

$$b_5 = -\left(\frac{c_1c_2q_hq_m}{D^2v^2} + \frac{P_1P_2P_3P_5\mu_m}{D} - \frac{P_1P_2P_4\mu_m}{D} - \frac{P_1P_3P_4\mu_m}{D} - \frac{P_2P_3P_4\mu_m}{D} + P_1P_2P_3P_4P_6\right)$$

$$b_6 = \frac{c_1c_2P_3q_hq_m}{D^2v^2} - \frac{P_1P_2P_3P_4\mu_m}{D}$$

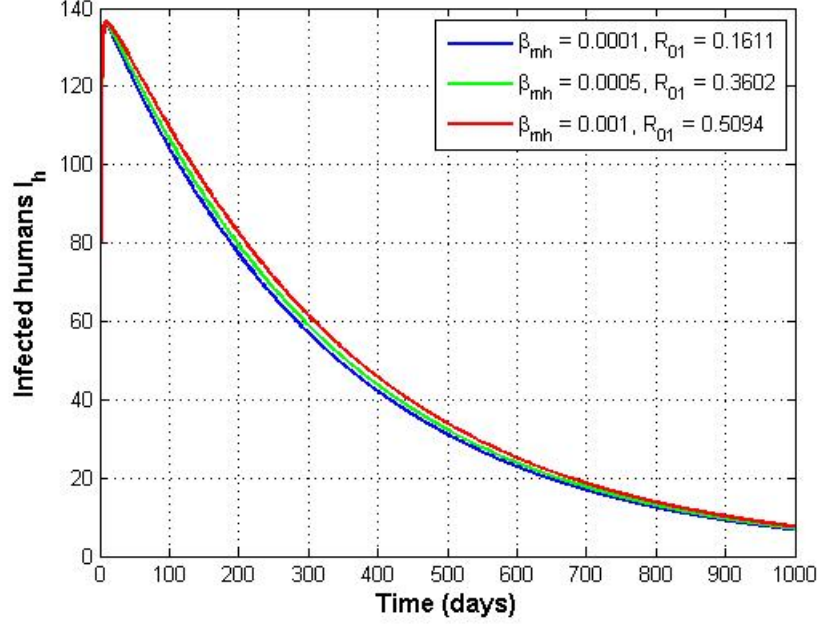


FIGURE 8. Time versus infected human

$$\text{and } P_1 = \frac{q_h + \mu_h}{v}, P_2 = \frac{\delta_h + v_h + \mu_h}{v}, P_3 = \frac{\alpha_h + \mu_h}{v}, P_4 = \frac{q_m + \mu_m}{D}, P_5 = P_6 = \frac{k - v}{D}$$

Also, considering the assertions and that $\lim_{\Psi} \rightarrow -\infty = +\infty$, the polynomial $p(\Psi)$ always has a negative real roots.

Therefore, for $R_{02}^2 = 1$, we obtain that $v_{min} = 0$, and then non-wave speed exists for $R_{02}^2 < 1$, the existence of 3 real roots depends on the value of v .

However, the minimal speed at the double root of the polynomial is $p(v_{min}) = p'(v_{min}) = 0$ Secondly, we consider the advection movement (i.e $k \neq 0$, k) appear adding the value of v , from the expression of the polynomial coefficients b_0, b_1, b_2, b_3, b_4 and b_5 . Hence, advection increases the wave speed when it is in the same direction as the wave front and decreases it when it is in the opposite direction.

Remark 3. The wave speed, v will be determine by estimating the fly speed of the mosquito per day which we term as diffusion (the D value). Therefore, for $R_{02}^2 = 1$, we obtain that $v_{min} = 0$, and then, non-wave speed exists. For $R_{02}^2 > 1$, the existence of two real roots depends on the value of v . For $v < v_{min}$, the roots are complex. For $v = v_{min}$, we have a double negative real root and for $v > v_{min}$ two negative real roots. When we consider the advection movement ($k \neq 0$), from the expression of the polynomial coefficients b_0, b_1, b_2, b_3, b_4 and b_5 , we can observe that k appears adding the value of v . Hence, advection increases the wave speed when it is in the same direction of the wave front and decreases it when it is in the opposite direction.

5.1. Numerical simulation of the wave equations. In this section, we present the numerical solution of the wave equations as shown in Table 3 below.

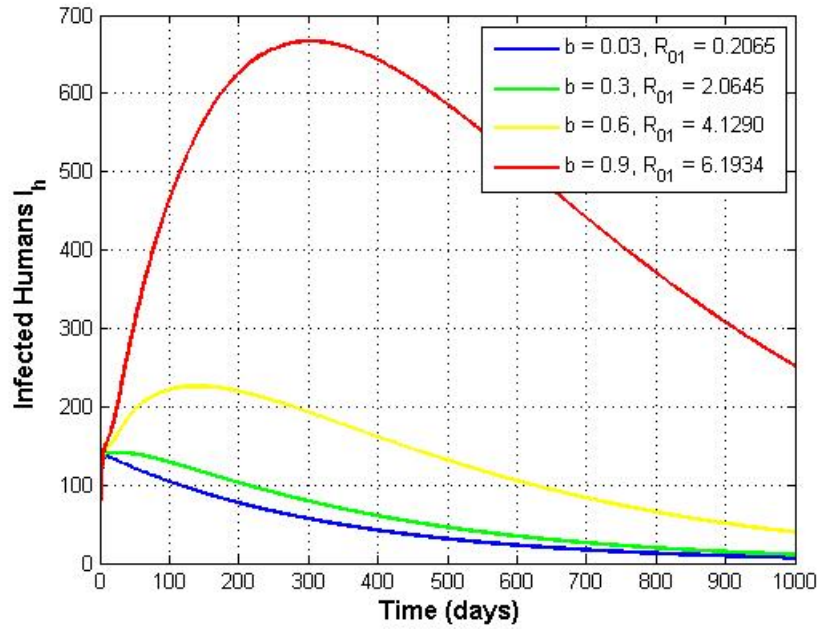


FIGURE 9. Time versus infected human

TABLE 3. Different velocity values with their respective roots of a polynomial $D = 0.125$ and $k = 0$

v	Ψ_1	Ψ_2	Ψ_3	Ψ_4	Ψ_5	Ψ_6	Ψ_7
0.1	-2.7385	-1.15031	0.0779698	1.79358	3.48606	4.44862	8.50242
0.3	-2.73749	-1.18434	0.0665686	0.905346	$1.56908 - 0.943076i$	$1.56908 + 0.943076i$	3.28506
0.6	-2.76433	-1.1591	0.0538016	0.0456375	$0.91639 - 0.797039i$	$0.91639 + 0.797039i$	2.31718
0.9	-2.78444	-1.12096	0.0447799	0.302723	$0.640594 - 0.697239i$	$0.640594 + 0.697239i$	2.10111

6. DISCUSSION

In Figure 5, we varied the biting or contact rate parameter, b , from 0.2/day to 0.9/day. This parameter indicates the contact rate between mosquitoes and the human population. The result shows that, at the lowest biting rate (i.e. $b = 0.2/\text{day}$), the infected human populations declined, while at the highest biting rate (i.e. $b = 0.9/\text{day}$), the infected human populations increased spontaneously and later declined. The long run decrease of the infected human population at different biting rate is due to those that recovered from the disease, died due to infection, and the natural death rate of the population. It is interesting to note from this result that if the contact rate between human populations and mosquito populations can be eliminated, there will be no malaria. However, this may sound impossible in an area that has vegetation with mosquitoes harbouring in them.

In Figure 6, we varied plant growth parameters, gm^2/day , from $0.1m^2/\text{day}$ to $0.9m^2/\text{day}$. We observed from the plot that the increase in the plant population leads to a more infected human population. This is so because, when there is more vegetation that attracts mosquito

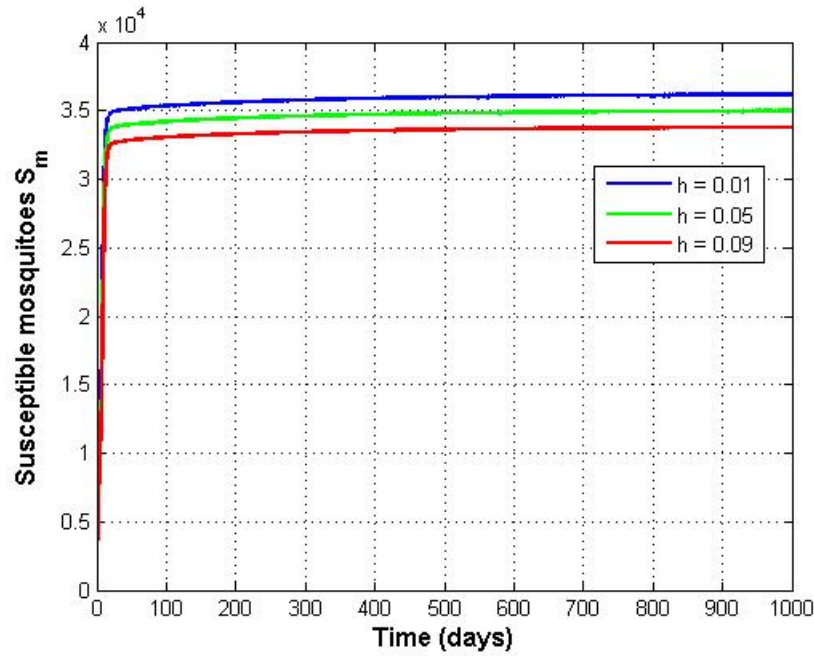


FIGURE 10. Time versus susceptible mosquito

into human environment, there will be more availability of mosquitoes in such an environment, and thereby leading to high human and mosquito contact as previously shown in Figure 5. This result may intuitively contradict the issue of ecological maintenance and protection, since the human environment may become inhabitable when all invasive plants are destroyed. From a scientific viewpoint, invasive plants that attract mosquito such as flowers, water lilies, Water hyacinths, Water lettuce, Taro, and Papyrus can be replaced with vegetation that serves as mosquitoes repellents such as Bee Balm, Rosemary, Catnip, Floss Flower, Garlic, Lavender, Lemon Balm, Lemongrass and Marigold to mention a few to maintain ecosystem balance.

To augment our claims in Figure 6, we varied the invasive plants' growth rate parameter, gm^2/day , from $0.1m^2/\text{day}$ to $0.9m^2/\text{day}$ in Figure 7. It was found that the higher the invasive plants' growth rate, the higher the availability of mosquitoes in the human environment. The issue of malaria burdens is more in the African region as they have the highest percentage of malaria burdens worldwide. African countries are characterized by huge mosquitoes and attracting vegetation. This is one of the key parameters that accelerate the malaria burden. The use of mosquito nets and insecticide spray may not have a great impact on malaria control in African countries, since people will not continue to sleep or stay inside mosquito nets from 6:00 pm to 6:00 am the following day. In this case, the issue of vegetation control is very paramount, if malaria burdens should be drastically reduced in African countries.

Figure 8 shows plots of the different transmission rates of malaria parasites from mosquitoes to humans, β_{mh} with their respective basic reproduction number, R_{01} . The infected human populations increased whenever more malaria parasites are injected into human blood, while the infected humans showed a decrease in population as a result of the reduction of

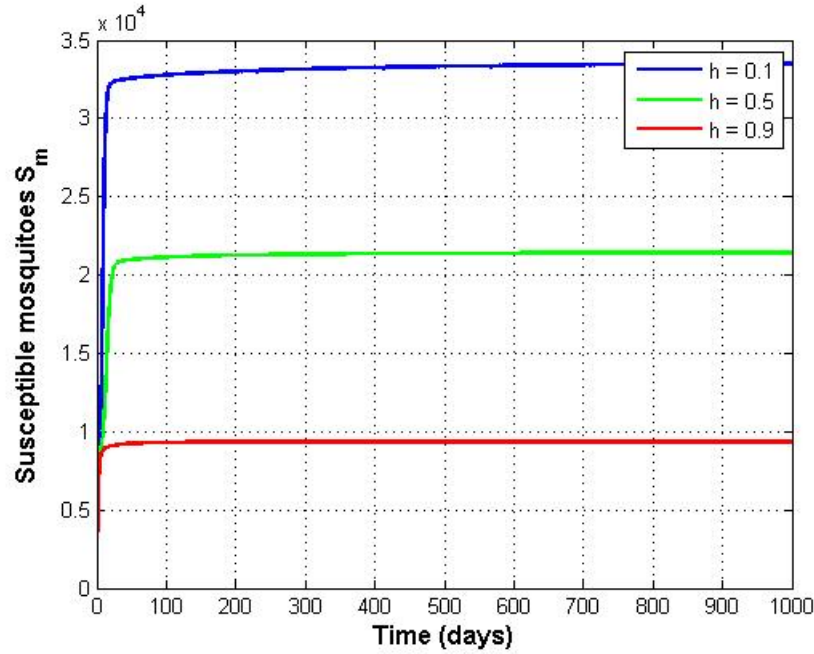


FIGURE 11. Time versus susceptible mosquito

malaria parasites injected into human blood. However, the result also informed us that the basic reproduction number increased due to the increased transmission rate of malaria parasites from mosquitoes to humans. However, in Figure 9, we showed the impact of the contact rate parameter, b of mosquitoes in human populations on the disease's basic reproduction number, R_{01} . This result is very crucial since it can predict and inform a decision on what rate of biting or contact rate between human and mosquito populations the disease will die down. In this figure, we can see that the higher the biting or contact rate, b of the mosquitoes, the higher the disease's basic reproduction number, R_{01} . It is also very important to note from this result that from $b = 0.3/\text{day}$ to $0.9/\text{day}$, the disease remained endemic as their respective basic reproduction number, R_{01} , continues to be greater than one. However, at $b = 0.03$, the value of the disease's basic reproduction number becomes 0.2065, which is less than one. It is important to seek this value of b so that the disease can be eliminated from the human population.

In Figure 10, we showed the impact of invasive plant or vegetation reduction due to deforestation and their natural death rate on susceptible mosquitoes' availability. To do this, the parameter, h , which indicates the reduction of invasive plant parameters varied from $0.01m^2/\text{day}$ to $0.09m^2/\text{day}$. The plots show that the higher the number of invasive plants reduction rate, the lower the availability of susceptible mosquitoes and vice versa. Figure 11 follows the same pattern as Figure 10. However, we used higher invasive plants reduction rate parameter, h (i.e. $0.1m^2/\text{day}$ to $0.9m^2/\text{day}$) than the previous figure. A similar interpretation is also applied to this figure. In Figure 12, we also varied the invasive plants or vegetation reduction rate, h from $0.1m^2/\text{day}$ to $0.8m^2/\text{day}$ to see how it impacts the invasive plants' population. The low invasive plants' reduction rate shows a higher invasive plants population and vice versa. This figure shown here to prove our claimed

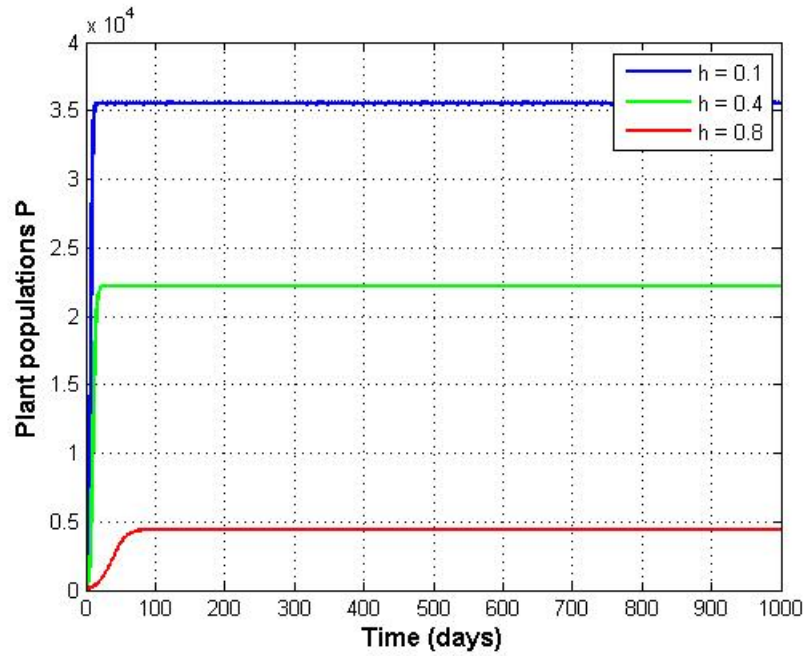


FIGURE 12. Time versus invasive plant

results in Figures 10 and 11. Figure 13 shows the plots of the infected human population, I_h versus the basic reproduction number, R_{01} . This plot shows evidence of the bifurcation phenomenon of the system of equations (3.1). Looking at the plot critically, it is observed that the curve equilibrium was reversed at the value $R_{01} = 1$. In Figure 14, we plotted the biting or contact rate parameter, b against basic reproduction number, R_{01} , the disease burden increases (at $b = 0.3/\text{day}$) unabatedly. This is to say that human and mosquito population contact rates have a high impact on disease prevalence. This result shows that the reduction of mosquitoes and human contact rates with the aid of plants reduction and the use of bed nets is pivotal to maintaining control over the disease spread.

Figure 15 is a plot of the transmission rate of malaria parasites from mosquitoes to the human population versus the disease's basic reproduction number, R_{01} . In this plot, we used the following parameters: values $g = 0.002m^2/\text{day}$, $K_p = 400m^2/\text{day}$, $\xi = 0.99/\text{day}$, $\gamma = 0.99/\text{day}$ in addition to the parameter values in Table 2. It can be observed that the disease transmission did not continue indefinitely as the disease's basic reproduction number remained less than one all through. This happened as a result of two major controls used here, which include: a reduction in invasive plants' growth rate, and an increase in bed net and its efficacy.

7. CONCLUSION

In this work, we developed a novel spatial non-linear mathematical model on the impact of vector control strategies on the dynamics of malaria transmission in invasive alien plants-dominated ecosystems. Three major vector control strategies are employed in this paper, which include: the control of invasive alien plants (Stone *et al.* 2018) and insecticide-treated bed-net and insecticide spray.

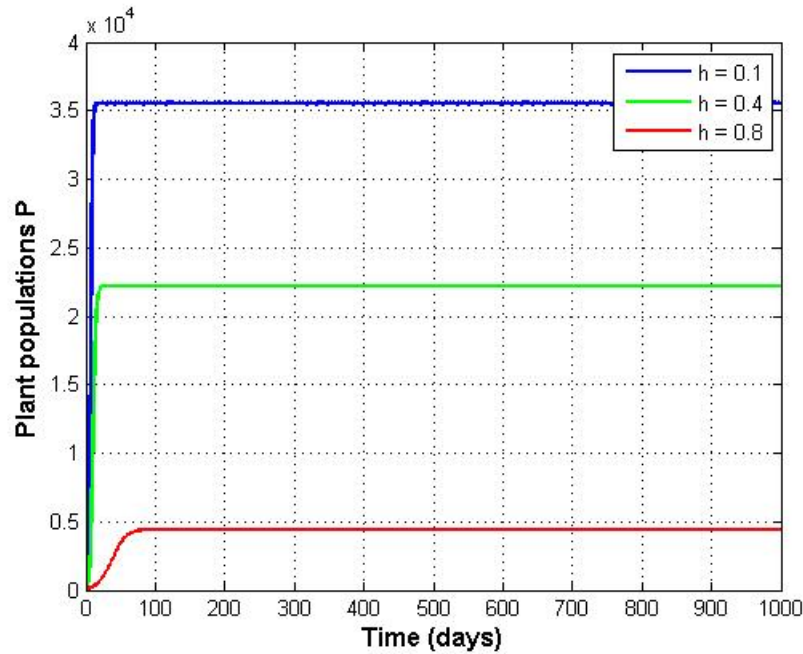


FIGURE 13. Time versus invasive plant

The most notable vector control strategy in this work is the control of invasive alien plants that serve as mosquitoes attractor and are thereby capable of increasing mosquitoes populations tremendously in the human environment. However, at the moment, there are too many mosquitoes in human habitats, the contact rate between mosquitoes and humans increases, as well as the increase of the transmission rate of malaria parasite infection from an infected female *Anopheles* mosquito to human.

The use of insecticide-treated bed-net becomes insignificant once mosquitoes are readily available in the human environment at all times because people only get into their insecticide-treated bed-nets at late hours. Also, the use of insecticide spray becomes a waste of resources since they are enough mosquitos' populations. The reason is that insecticide spray kills mosquitoes within an applicable area for some specific hours after application and concentration later become ineffective to kill further influx of mosquitoes. The continuous influx of mosquitoes into such environment may render insecticide application useless and effortless.

In this work, we go beyond considering just human (host) population and mosquito (vector) population as many mathematical models of malaria authors normally consider the disease model with the existing model compartment and with just introduction of the new parameter(s) into some compartments of their model equations. However, in this paper, we critically considered the issue of invasive alien plants or vegetation that serve as shelters for mosquitoes' propagation and reproduction at a faster rate. Due to this surveillance, we included invasive alien plants as a compartment between human compartments and mosquito compartment and showed how these invasive alien plants interact with vector populations.

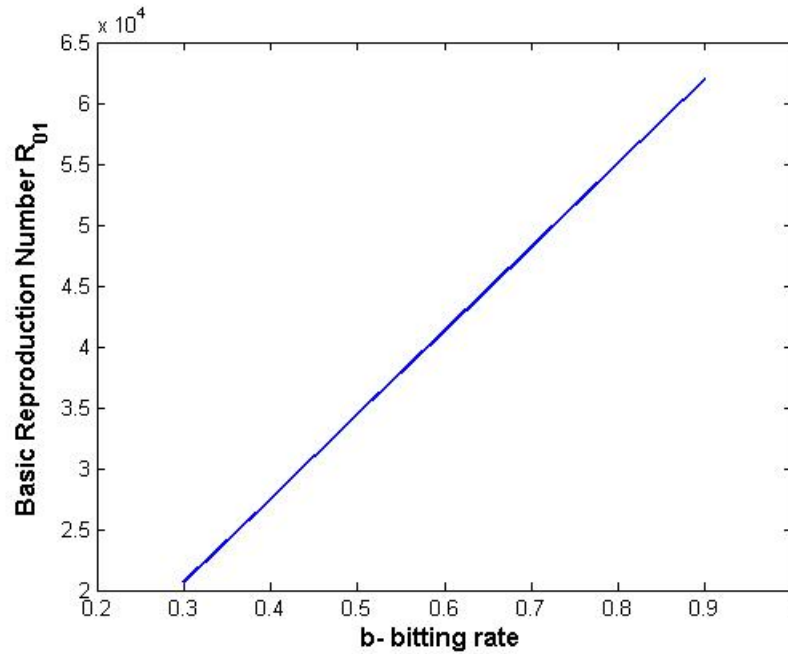


FIGURE 14. Time versus basic reproduction number

The model system was analyzed for many possible equilibria. Three equilibria were obtained from system (3.1), namely, two disease-free equilibria and one disease endemic equilibrium. The two disease-free equilibria, E_1 and E_2 , are respectively the cases where there are invasive alien plants in the human environment. The E_1 equilibrium shows the presence of mosquitoes from the invasive alien plants and those that are already in the human environment. In this equilibrium, none of the mosquitoes are infected with the malaria parasite and there is no malaria. Also, the equilibrium, E_2 without invasive alien plants has fewer mosquitoes in the human environment due to the absence of invasive alien plants. The third equilibrium, E_3 , shows the interaction between the infected mosquitoes and human populations. Malaria disease is observed and remains in as much as both the infected and susceptible human populations continue to live together with mosquitoes present in their environment. The three equilibria, E_1 , E_2 and E_3 were also analysed for their stability behaviour. It was found that their stability depends on the basic reproduction number of the disease: R_{01} for E_1 and E_3 and R_{02} for E_2 . The E_1 and E_2 equilibria are locally asymptotically stable provided R_{01}^2 and R_{02}^2 are less than one respectively while the global stability of E_3 must satisfy the value of R_{01}^2 to be greater than one. To avoid talking too much about the mathematics of these equilibria, we simply thoroughly explain the terminology. Those with mathematics bias can check for the equilibria and the basic reproduction number equations for easy understanding. However, on a general note, the basic reproduction number is the number of infections one infected person can cause during the time of his/her infectiousness. Once the basic reproduction number value is greater than one, it means that the disease will thrive.

The major contribution of this basic reproduction number is to inform us about what parameter value we need to reduce that will make $R_0(R_{01}, R_{02})$ less than one. Looking at the

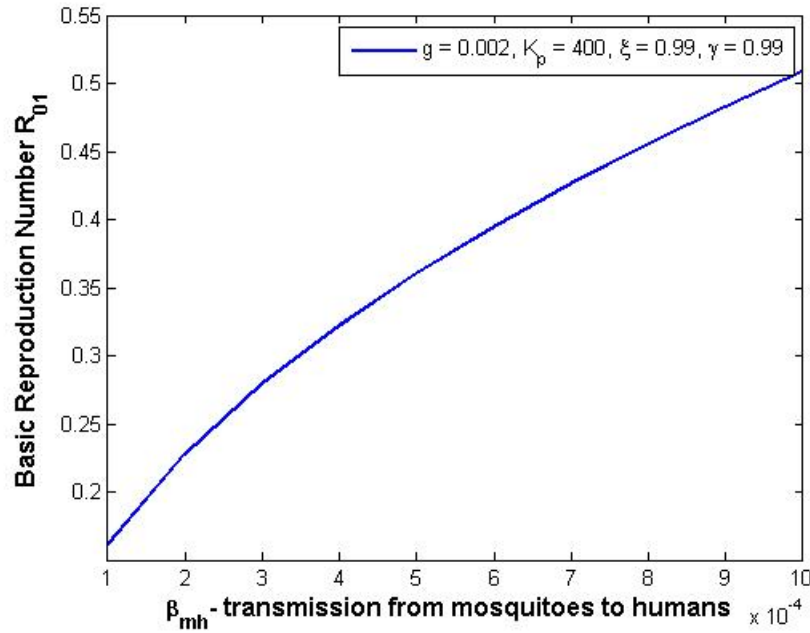


FIGURE 15. Time versus basic reproduction number

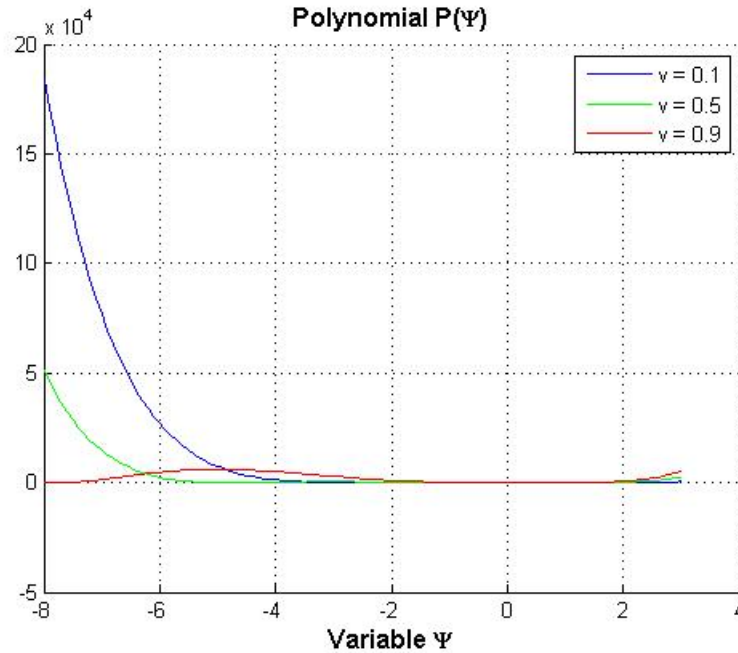
basic reproduction number equations critically, you will find out that not all the parameters in the equations lead to host and vector interaction. The major parameters here are biting rate, transmission from mosquitoes to humans, and the invasive alien plants' growth rate. Decreasing these parameter values leads to R_{01}^2 being less than one. Most importantly, decreasing plant growth rate leads to a decrease in plant populations, while decreasing plant population leads to a decrease in mosquito availability in the human environment. Also, decreasing mosquito availability in the human environment will lead to a decrease in biting rate while a decrease in biting rate leads to a decrease in malaria transmission rate.

The equilibrium, E_3 was also analyzed for possible bifurcation phenomenon. We found that system (3.1), exhibits a backward bifurcation phenomenon at E_3 equilibrium. The result shows the possibility of some urban cities in African countries without or with a few invasive alien plants are free from malaria, while villages or rural areas with dense invasive alien plants are malaria-endemic regions.

Moreover, we present a traveling wave equations (5.1) to determine the behaviour of the mosquitoes population from the invasive alien plants to human environments and how they return to the invasive alien plants during the day. We obtained the polynomial equation (5.4) through Jacobian methods of linearization.

In carrying out the numerical simulation of system (3.1), we can provide answers to questions raised by (Stone *et al.* 2018) in review work on how the control of aliens invasive plants reduce malaria transmission. Our numerical simulation was designed to provide comprehensive answers to those salient questions posed in their work.

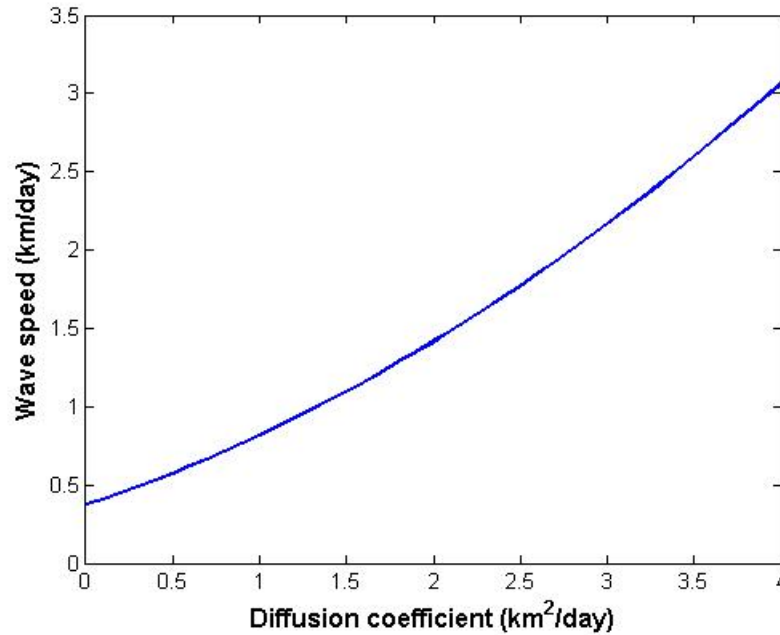
The first question is: do invasive alien plants have a positive influence on the rate of malaria transmission? We saw from some plots in this work that invasive alien plants have a positive influence on the rate of malaria transmission. How? Paying close attention

FIGURE 16. Wave speed at different values of v

to some of our graphs where we varied the plants' growth rate and plotted the infected human population over time, we found that people get infected more with an increase in invasive alien plants growth rate, r . Also, considering the invasive alien plants' destruction rate, h , we found that the susceptible mosquito population decreases as the parameter, h increases. Mosquitoes become more alarming when the invasive alien plants produce nectar that mosquitoes feed on in the daytime. However, we do not capture explicitly, the invasive alien plants' nectar production in our model. Intuitively, invasive alien plants' nectar serves as an attraction to mosquitoes and also serves as a shelter for them.

Another notable question that was also raised is how do mosquitoes' interactions with invasive alien plants cause differences in malaria transmission? This question is somehow similar to the first question we just responded to previously. However, in this question, we are expected to provide solutions to some issues raised in our responses to the first question. In this case, our aim will be on how to manage these so-called invasive alien plants since they contribute greatly to malaria transmission. We have responded previously that the increase of mosquito availability in the human environment increases both the biting rate and the transmission rate parameters. This sounded more of a theory but we were able to verify this from our numerical simulation. We therefore take a step further to investigate the impact of these parameters (b, β_{mh}, r and h) on the disease's basic reproduction number. We used the baseline values parameter in Table 2 and we found that the basic reproduction number was above 200. By assigning relatively smaller values to bite rate, b and the transmission rate parameter, β_{mh} , we obtained the basic reproduction value for a number less than one.

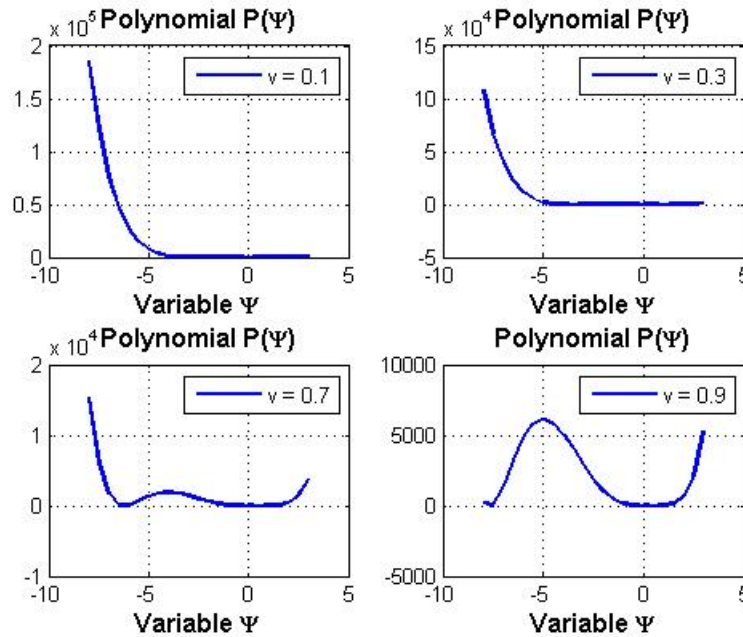
The question now is how do we optimally manage these invasive alien plants without jeopardizing their usefulness to both aquatic and terrestrial ecosystems? The authors,

FIGURE 17. Wave speed at different values of v

(Stone *et al.* 2018) have suggested many methods, which include: manual, mechanical, chemical, and biological methods, of these said plants' removal. The use of a manual method such as uprooting and clearing the environment with the use of cutlass and hoes seems to be an effective method since some needed plants will be preserved. However, in an area with the aggressive growth of these plant species, the manual method may seem too slow to embark on. The mechanical method of control involves the use of tractors, bulldozers, and excavators, to mention a few for clearing and uprooting such plants without considering some species of other plants that may be needed. This method also has an issue with landscape change as this can lead to soil erosion.

The use of pathogens, insects, and mites as a biological method to suppress plants' vigours, slow plant infestation, and reduce seed production will bring about agricultural farms to be less productive as this method may also result to crop loss and economic crisis as many crops will be disturbed as well. The use of the chemical method is quick and cheap to embark on but it has a lot of environmental hazard impacts. The issue of malaria would have been a thing of the past now if DDT (dichlorodiphenyltrichloroethane) was sustained for a long time. Its effects on environmental pollution and risks have led to its application stoppage by chemical use law enforcement agencies. The aquatic environment will get polluted by chemical concentrations and an attempt for a human to consume such aquatic species will result in chemical bio-accumulation and bio-magnification. Recently, Achema *et al.* (2021) found that the use of chemicals/pesticides in an aquatic environment is detrimental to the survival of aquatic biological species and also has negative effects on human health.

On the whole, weighing the merits and demerits of each of the methods, we may still not have a sound ecological setting. In this paper, our most important management of these

FIGURE 18. Subplots of wave speed at different values of v

invasive alien plants (*Prosopis juliflora*, *Parthenium hysterophorus*, *Senna didymobotrya*, and *Tecoma* to mention a few) recommendations is to use both manual and mechanical methods to destroy them where needed and replace them by planting mosquitoes repellents plants such as Bee balm, Rosemary, Catnip, Floss flower, Garlic, Lavender, Lemon balm, Lemongrass, and Marigold.

We also carried out a traveling wave solution simulation. Equation (5.4) was simulated and it was found to be unstable at every given value of the wave velocity. However, we noticed changes in the system equilibrium at higher wave velocity values ($v = 0.7m/s$ and $v = 0.9m/s$) with both real and imaginary eigenvalues. This is to show that the system will remain unstable as far as there are invasive alien plants in the human environment (see Table 3).

8. ACKNOWLEDGEMENTS

The authors wish to acknowledge anonymous reviewers. We also wish to thank Prof. Daniel Okuonghae, Mathematics Department, University of Benin, Benin-City, Nigeria for his valuable encouragement and discussions we had at the development phase of the model.

REFERENCES

- [1] Achema, K.O. Okuonghae, D. Tongo, I. (2021). Dual-level toxicity assessment of biodegradable pesticides to aquatic species. *Ecological Complexity*. 45: 1-34.
- [2] Agosto, F.B. Gumel, A.B. Parham, P.E. (2015). Qualitative assessment of the role of temperature variation on malaria transmission dynamics. *J. Biol. Syst.* 24, 1-34.

- [3] Artzy-Randrup, Y., Alonso, D., Pascual, M. (2010). Transmission Intensity and Drug Resistance in Malaria Population Dynamics: Implications for Climate Change. *PLoS ONE*. 5(10), e13588 doi:10.1371/journal.pone.0013588.
- [4] Castillo-Chavez, C., Song, B. (2004). Dynamical model of tuberculosis and their applications. *Math. Biosci. Eng.* 1(2), 361–404
- [5] Cjl, M., Ortblad, K.F., Guinovart, C., Lim, S.S., Wolock, T.M., Roberts, D.A. (2014). Global, regional and national incidence and mortality for HIV, tuberculosis, and malaria during 1990-2013: a systematic analysis for the global burden of disease study 2013. *Lancet*. 384(9947): 1005–10070
- [6] Diabaté, A. B., Sangaré, B. and Koutou, O. (2022). Mathematical modeling of the dynamics of vector-borne diseases transmitted by mosquitoes : taking into account aquatic stages and gonotrophic cycle, *Nonauton. Dynamical System*, 9: 205-236
- [7] Davis, T., Kline, D., Kaufman, P.(2016). *Aedes albopictus* (Diptera: Culicidae) oviposition preference as influenced by container size and *Buddleja davidii* plants. *Journal of Medical Entomol.* 53, 273–278
- [8] Gardner, A.M., Muturi, E.J., Overmier, L.D., Allan, B.F. (2017). Large-scale removal of invasive honey-suckle decreases mosquito and avian abundance. *EcoHealth*. 14(4), 750–761
- [9] Hien, D., Dabiré, K., Roche, B., Diabaté, A., Yerbanga, R.S., Cohuet, A. (2016). Plant-mediated effects on mosquito capacity to transmit human malaria. *PLoS Pathog.* 12(8), e1005773
- [10] Julius, T., Senelani, D.H. Farai, N. (2014). A mathematical model for the transmission and spread of Drug sensitive and Resistant Malaria strains within a Human population. 4: 1-12
- [11] Koutou, O. Diabaté, A. B. and Sangaré, B. (2023). Mathematical analysis of the impact of the media coverage in mitigating the outbreak of COVID-19, *Math. Comput. Simul.* 05: 600 - 618
- [12] Kroeger, I., Liess, M., Dziock, F., Duquesne, S. (2013). Sustainable control of mosquito larvae in the field by the combined actions of the biological insecticide Bti and natural competitors. *Vector Ecol.* 38: 82–89
- [13] Mack, R., Smith, M. (2011). Invasive plants as catalysts for the spread of human parasites. *NeoBiota.*, 9, 13–29
- [14] Müller, G.C., Junnila, A., Traore, M., Traore, S.F., Doumbia, S., Sissoko, F. (2017). The invasive shrub *Prosopis juliflora* enhances the malaria parasite transmission capacity of *Anopheles* mosquitoes: a habitat manipulation experiment. *Malaria Journal*. 16(237)
- [15] Muturi, E.J., Gardner, A.M., Bara, J.J. (2015). Impact of an alien invasive shrub on ecology of native and alien invasive mosquito species (Diptera: Culicidae). *Environ Entomol.* 44, 1308–1315
- [16] Nkya, T.E., Akhouayri, I., Poupardin, R., Batengana, B., Mosha, F., Magesa, S.(2014). Insecticide resistance mechanisms associated with different environments in the malaria vector *Anopheles gambiae*: a case study in Tanzania. *Malaria Journal*, 13-28
- [17] Nwankwo, A., Okuonghae, D. (2019). A mathematical model for the population dynamics of malaria with a temperature dependent control. *Foundation for Scientific Research and Technological Innovation*, Springer, 1-30
- [18] Okuneye, K., Gumel, A.B. (2015). Analysis of a temperature and rainfall dependent model for malaria transmission Dynamics. *Math. Bios.* <https://doi.org/10.1016/j.mbs.2016.03.013>
- [19] Raghavendra, K., Barik, T.K., Niranjana-Reddy, B.P., Sharm, P., Dash, A.P. (2011). Malaria vector control: from past to future. *Parasitol Res.* 108, 757–759
- [20] Ranson, H., N'Guessan, R., Lines, J., Moiroux, N., Nkuni, Z., Corbel, V. (2011). Pyrethroid resistance in African anopheline mosquitoes: what are the implications for malaria control? *Trends Parasitol.* 27, 91–98
- [21] Resmawan, J. (2017). SEIRS-SEI Model of Malaria Disease with Application of Vaccines and Anti-Malarial Drugs. *IOSR Journal of Mathematics (IOSR-JM)* 3(4): 85–91 doi: 10.9790/5728-1304028591
- [22] Shackleton, R.T., Abr, W., Aool, W., Pratt, C. (2017). Distribution of the invasive alien weed, *Lantana camara*, and its ecological and livelihood impacts in eastern Africa. *African Journal Range Forage Sci.* 34: 1–11.
- [23] Stone, C.M., Witt, A.B.R., Walsh, G.C., Foster, W.A., Murphy, S.T. (2018). Would the control of invasive alien plants reduce malaria transmission? A review. *Parasites and Vectors.* 11(76): 1-18 doi: 10.1186/s13071-018-2644-8
- [24] Takoutsing, E., Temgoua, A., Yemele, D. Bowong, S. (2019). Dynamics of an Intra-Host model of malaria with periodic Antimalaria Treatment. *International Journal of Non-Linear Science*, 3(27):148-164
- [25] Titus O.O., Rachel W.M. and Livingstone S.L. (2018). Mathematical model for the in-host malaria dynamics subject to malaria vaccines, *Letters in Biomathematics*, 5(1): 222-251 doi: 10.1080/23737867.2018.1526132
- [26] Tumwine, J. Mugisha, V.T. Luboobi, L.S. (2017). A Mathematical model for the dynamics of malaria in a human host and mosquito vector with temporary immunity. *Applied Mathematics and Computation.* 189(20), 1953-1965

- [27] Vanessa, S. and Norberto, A. M. (2019). Modelling the Spatial Spread of Chagas Disease. *Bulletin of Mathematical Biology*, Springer, 22: 1-44
- [28] Van den Driessche, P., Watmough, J. (2008). Reproduction numbers and sub-threshold endemic equilibria for compartmental models of disease transmission. *Math. Biosci.* 180, 29-48
- [29] World Health Organisation (2021). World Malaria Report. http://www.who.int/malaria/publications/world_malaria_report_2014/report/en/. Accessed 10 May 2021
- [30] World Health Organisation (2022). World Malaria Report. http://www.who.int/malaria/publications/world_malaria_report_2021/report/en/. Accessed 13 June 2022
- [31] Zadoki, T., LivingStone, S. L. Joseph, S. (2017). Mathematical modelling of the in-host dynamics of malaria and the effects of treatment. *Journal of mathematics and computer Science.* 17: 1-21
- [32] Zhu, L., Marshall, J.M., Qualls, W.A., Schlein, Y., McManus, J.W., Arheart, K.L. (2015). Modelling optimum use of attractive toxic sugar bait stations for effective malaria vector control in Africa. *Malaria Journal.* 14(492).

CHARITY JUMAI ALHASSAN

DEPARTMENT OF MATHEMATICS,, EDO STATE UNIVERSITY, UZUAIKUE,, AUCHI OKENE ROAD, IYAHMO, EDO, NIGERIA.

Email address: charity.alhassan@edouniversity.edu.ng

KENNETH OJOTOGBA ACHEMA

DEPARTMENT OF MATHEMATICS,, JOSEPH SARWUAN TARKA UNIVERSITY, MAKURDI, NORTH BANK, MAKURDI 2373, BENUE, NIGERIA

Email address: kennethachema@gmail.com